

# ON CURVATURE-AIDED INCREMENTAL AGGREGATED GRADIENT METHODS

HOI-TO WAI , WEI SHI , CÉSAR A. URIBE , ANGELIA NEDIĆ , AND ANNA SCAGLIONE\*

**Abstract.** This paper studies an acceleration technique for incremental aggregated gradient methods which exploits *curvature* information for solving strongly convex finite sum optimization problems. These optimization problems of interest arise in large-scale learning applications relevant to machine learning systems. The proposed methods utilizes a novel curvature-aided gradient tracking technique to produce gradient estimates using the aids of Hessian information during computation. We propose and analyze two curvature-aided methods — the first method, called curvature-aided incremental aggregated gradient (CIAG) method, can be developed from the standard gradient method and it computes an  $\epsilon$ -optimal solution using  $\mathcal{O}(\kappa \log(1/\epsilon))$  iterations for a small  $\epsilon$ ; the second method, called accelerated CIAG (A-CIAG) method, incorporates Nesterov’s acceleration into CIAG and requires  $\mathcal{O}(\sqrt{\kappa} \log(1/\epsilon))$  iterations for a small  $\epsilon$ , where  $\kappa$  is the problem’s condition number. Importantly, the asymptotic convergence rates above are the same as those of the full gradient and accelerated full gradient methods, respectively, and they are *independent* of the number of component functions involved. The proposed methods are significantly faster than the state-of-the-art methods, especially for large-scale problems with a massive amount of data.

**Key words.** incremental gradient method, Hessian, second order approximation

**AMS subject classifications.** 90C06, 90C25, 90C30

**1. Introduction.** Consider a finite sum optimization problem with  $m$  component functions and a  $d$ -dimensional decision variable:

$$(1.1) \quad \min_{\boldsymbol{\theta} \in \mathbb{R}^d} F(\boldsymbol{\theta}) := \sum_{i=1}^m f_i(\boldsymbol{\theta}) .$$

The above problem is motivated by the so-called empirical risk minimization formulation where we are learning a parameter  $\boldsymbol{\theta}$  from a finite set of data. In particular, the component function  $f_i(\boldsymbol{\theta})$  represents the statistical mismatch between  $\boldsymbol{\theta}$  and the  $i$ th piece of data collected. As such, the aim of (1.1) is to learn the optimal parameter, denoted as  $\boldsymbol{\theta}^*$ , that minimizes the statistical mismatch between the distribution parameterized by  $\boldsymbol{\theta}$  and  $m$  available data points; see [30, 8].

This paper focuses on the case of *large-scale optimization* when  $m \gg 1$ . In particular, we are interested in the setting for (1.1) when each of the component function  $f_i(\boldsymbol{\theta})$  is twice continuously differentiable and the sum function  $F(\boldsymbol{\theta})$  is strongly convex. Despite that (1.1) is a strongly convex problem, the difficulty with solving it lies in the overwhelming size of  $m$ , which prohibits us from even applying simple first order methods. For example, the *full gradient* (FG) requires the recursion: let  $\gamma > 0$  be a step size,

$$(1.2) \quad \boldsymbol{\theta}^{k+1} = \boldsymbol{\theta}^k - \gamma \sum_{i=1}^m \nabla f_i(\boldsymbol{\theta}^k) ,$$

that involves a computation cost of  $\mathcal{O}(md)$  floating point operations (FLOPS) per iteration to compute the sum of  $m$  gradient vectors. As  $m \gg 1$ , this is undesirable from a practical standpoint. To this end, a popular yet powerful approach is to adopt the so-called *incremental* (or stochastic) methods where only one of the component functions, e.g., the  $i_k$ th one,  $f_{i_k}(\boldsymbol{\theta})$ , is explored at the  $k$ th iteration. Examples include the incremental gradient (IG) [6], incremental aggregated gradient (IAG) [7, 29, 16] methods when  $i_k$  is deterministic; and the stochastic gradient (SG) [25], stochastic average gradient (SAG) [27], SAGA [11], stochastic variance reduced gradient (SVRG) [32] methods when  $i_k$  is chosen randomly. Furthermore, related work can be found in [19, 28] for the case with non-convex functions; in [17] for the case of primal-dual optimization; in [21, 22] for the case with non-smooth functions.

---

\*H.-T. Wai, W. Shi, A. Nedić and A. Scaglione are with the School of ECEE, Arizona State University, Tempe, AZ, USA. E-mails: {htwai, wshi36, Angelia.Nedich, Anna.Scaglione}@asu.edu. C. A. Uribe is with the CSL, University of Illinois Urbana Champaign, Champaign, IL, USA. E-mail: cauribe2@illinois.edu. Preliminary version of this work has been presented at the 55th Annual Allerton Conference on Communication, Control, and Computing in October, 2017 [31].

	Storage	Comp.	# iterations to $\epsilon$ -optimal solution
IAG [7]	$\mathcal{O}(md)$	$\mathcal{O}(d)$	$\mathcal{O}(m \kappa(F) \log(1/\epsilon))$ [worst-case]
SAG [27]	$\mathcal{O}(md)$	$\mathcal{O}(d)$	$\mathcal{O}(\max\{\kappa(F), m\} \log(1/\epsilon))$ [expected]
SAGA [11]	$\mathcal{O}(md)$	$\mathcal{O}(d)$	$\mathcal{O}((\kappa(F) + m) \log(1/\epsilon))$ [expected]
SVRG [32]	$\mathcal{O}(d)$	$\mathcal{O}(d)$	$\mathcal{O}((\kappa(F) + m) \log(1/\epsilon))$ [expected]
AccSVRG [24]	$\mathcal{O}(d)$	$\mathcal{O}(d)$	$\mathcal{O}((m\sqrt{\kappa(F)} + m) \log(1/\epsilon))$ [expected]
Katyusha [2]	$\mathcal{O}(d)$	$\mathcal{O}(d)$	$\mathcal{O}((\sqrt{m\kappa(F)} + m) \log(1/\epsilon))$ [expected]
Catalyst-SAG [18]	$\mathcal{O}(md)$	$\mathcal{O}(d)$	$\mathcal{O}(\sqrt{m\kappa(F)} \log(1/\epsilon))$ [expected]
IQN [20]	$\mathcal{O}(md^2)$	$\mathcal{O}(d^2)$	$\mathcal{O}(m)$ , <i>i.e.</i> , super-linear [worst-case]
NIM [26]	$\mathcal{O}(md + d^2)$	$\mathcal{O}(d^3)$	$\mathcal{O}(m)$ , <i>i.e.</i> , super-linear [worst-case]
SVRG2 [13]	$\mathcal{O}(d^2)$	$\mathcal{O}(d^2)^\dagger$	$\mathcal{O}(\kappa(F) \log(1/\epsilon) + m)^\dagger$ [expected]
CIAG	$\mathcal{O}(md + d^2)$	$\mathcal{O}(d^2)$	$\mathcal{O}(\kappa(F) \log(1/\epsilon) + m)$ [worst-case]
A-CIAG	$\mathcal{O}(md + d^2)$	$\mathcal{O}(d^2)$	$\mathcal{O}(\sqrt{\kappa(F)} \log(1/\epsilon) + m)$ [worst-case]

TABLE 1

Comparison of different methods for the strongly convex problem (1.1). The second column is the memory required for the working variables. The third column is the per iteration computation complexity in FLOPS. The last column is the (expected or worst-case) number of iterations to reach an  $\epsilon$ -optimal solution, note that SVRG, AccSVRG, Katyusha, SVRG2 methods require recomputing the full gradient at every epoch. The constant  $\kappa(F)$  is the condition number of  $F(\theta)$  [cf. see (1.3) and (1.4) for the definition]. Note that the rates presented for the last five methods are asymptotic, *i.e.*, they hold only when  $\epsilon \rightarrow 0$ .  $^\dagger$  This rate is achieved by setting the number of iterations per epoch as  $\kappa(F)$  [cf. Proposition 1 of [13]].

For the convergence rate of incremental methods when applied to strongly convex problems, linear convergence can be achieved via the variance reduction technique, *e.g.*, in [32, 11, 27], where the past gradients are aggregated to estimate the current gradient. Nevertheless, these methods require  $k = \Omega(m \log(1/\epsilon))$  iterations to guarantee that they compute an  $\epsilon$ -optimal solution  $\theta^k$  satisfying  $F(\theta^k) - F(\theta^*) \leq \epsilon$ . In fact, recent work [1, 3, 17] showed that the dependence on  $m$  is necessary for incremental methods whose updates are linear combinations of the first order information.

To improve the convergence rate of incremental methods, a recent direction is to adopt ideas of second-order optimization. Examples include [14, 26, 20] which extended Newton and quasi-Newton methods to the incremental setting, resulting in NIM [26] and IQN [20]. Interestingly, these works demonstrated that at the expense of additional storage or computation cost, it is possible to achieve local *superlinear* convergence. A comparison of the state-of-the-art methods are summarized in Table 1.

**Contributions.** This paper proposes a general procedure for accelerating incremental gradient methods with second order information. Our contributions are:

- We propose a *curvature-aided gradient tracking* technique for accelerating incremental gradient methods using Hessian information. Specifically, by applying the Taylor expansion on the component functions' gradients, we derive a new gradient estimator whose error depends on the *squared* version of the optimality gaps. The tracking accuracy can be significantly improved when the optimality gap is small.
- Based on our new gradient tracking technique, we propose two incremental gradient methods, called Curvature-aided Incremental Aggregated Gradient (CIAG) method and Accelerated CIAG (A-CIAG) method. The proposed methods require only  $\mathcal{O}(md)$  storage cost and  $\mathcal{O}(d^2)$  computation cost per iteration. When  $\epsilon$  is small, we show that the CIAG method (*resp.* A-CIAG) requires  $k = \mathcal{O}(\kappa(F) \log(1/\epsilon))$  (*resp.*  $\mathcal{O}(\sqrt{\kappa(F)} \log(1/\epsilon))$ ) iterations to achieve an  $\epsilon$ -optimal solution with  $F(\theta^k) - F(\theta^*) \leq \epsilon$  [cf. Theorem 4.4 and 4.5]. Importantly, the attained rates are independent of the number of component functions,  $m$ , and they are on par with methods that evaluate the exact gradient at each iteration.

- Unlike previous work which focuses on the *expected convergence rates* for incremental/stochastic methods, we analyze the *worst case convergence rate* of the proposed methods under the assumption of bounded delay [cf. Assumption 4.1]. Typically the worst case rate of an incremental gradient method may exhibit a worse dependence on  $m$  [cf. comparing IAG and its stochastic version SAG in Table 1]. Our analysis does not demonstrate such artifact. This is attributed to the use of curvature-aided gradient tracking. Importantly, we remark that our result extends naturally for a parallel computation setting with asynchronous workers, e.g., [4].
- As a by-product of our analysis, we prove the linear convergence for two *non-linear* inequalities [cf. Proposition 4.10 and 4.11]. Our result reveals that convergence depends on the initialization, and the trajectory of convergence can be divided into two phases — the initial phase that exhibits a slow linear rate; and the asymptotic phase that exhibits linear convergence of a fast rate.

It is worth mentioning that recently in [13] the authors proposed a method that incorporates Hessian information to accelerate SVRG method, giving the SVRG2 method. The authors developed a number of approximation techniques to reduce the per iteration complexity from  $\mathcal{O}(d^2)$  to  $\mathcal{O}(d)$ . The best convergence rates achieved therein match that of the FG method, *i.e.*, the same as the CIAG method. However, we note that SVRG2 re-computes the full Hessian at the beginning of each epoch. This costs  $\mathcal{O}(md^2)$  FLOPS and the cost is negligible only when the epochs are long, e.g., when the epoch lengths are in the same order as  $m$ . Moreover, to attain the best convergence rate, SVRG2 requires setting the epoch length as  $\kappa(F)$ . This implies that SVRG2 is effective (e.g., compared to SAG) when  $\kappa(F) = \Omega(m)$ , *i.e.*, problems with poor condition numbers. In contrast, the CIAG and A-CIAG methods are effective regardless of the condition number.

**Organization.** The paper is organized as follows. Section 2 studies incremental methods as algorithms with *gradient tracking* and introduces the curvature-aided gradient tracking technique. Section 3 describes the proposed CIAG and A-CIAG methods, and discusses the implementation issues. Section 4 provides the main convergence results. Section 5 demonstrates the efficacy of the proposed methods using numerical experiments. Detailed proofs can be found in the appendix.

**Notations.** Unless otherwise specified, we denote by  $\|\cdot\|$  the standard Euclidean norm. A function  $f : \mathbb{R}^d \rightarrow \mathbb{R}$  is  $L$ -smooth if

$$(1.3) \quad f(\theta') \leq f(\theta) + \langle \nabla f(\theta), \theta' - \theta \rangle + \frac{L}{2} \|\theta' - \theta\|^2, \quad \forall \theta, \theta' \in \mathbb{R}^d,$$

and it is  $\mu$ -strongly convex if

$$(1.4) \quad f(\theta') \geq f(\theta) + \langle \nabla f(\theta), \theta' - \theta \rangle + \frac{\mu}{2} \|\theta' - \theta\|^2, \quad \forall \theta, \theta' \in \mathbb{R}^d,$$

Define  $\kappa(f) := L/\mu$  as the condition number of  $f$ . Moreover,  $f$  has an  $L_H$ -Lipschitz continuous Hessian if

$$(1.5) \quad \|\nabla^2 f(\theta') - \nabla^2 f(\theta)\| \leq L_H \|\theta' - \theta\|, \quad \theta, \theta' \in \mathbb{R}^d,$$

where the norm on the left hand side is the matrix norm induced by Euclidean norm. For a non-negative scalar sequence  $\{a^{(k)}\}_{k \geq 1}$ , we say that it converges linearly at a rate  $\rho$  if the sequence satisfies  $\lim_{k \rightarrow \infty} a^{(k+1)}/a^{(k)} = \rho$ , where  $0 \leq \rho < 1$ . We use standard Bachmann-Landau notations for asymptotic quantities:  $a^{(k)} = \mathcal{O}(f^{(k)})$  (*resp.*  $a^{(k)} = \Omega(g^{(k)})$ ) implies that there exists  $k_0 \in \mathbb{Z}_+$  and non-negative constant  $C_1$  (*resp.*  $C_2$ ) such that  $a^{(k)} \leq C_1 f^{(k)}$  (*resp.*  $a^{(k)} \geq C_2 g^{(k)}$ ) for all  $k \geq k_0$ .

**2. Gradient Tracking in Incremental Methods.** Before we delve into the technical details, we provide a high-level review of the *variance-reduced* incremental/stochastic gradient methods as applying forms of *gradient tracking* to avoid computing the costly full gradient during iterations.

To set up the notations, let  $i_k \in \{1, \dots, m\}$  be the component function index selected at the  $k$ th iteration, e.g., a simple rule is to use the cyclic rule as  $i_k = (k \bmod m) + 1$ , or for stochastic methods, we may choose  $i_k \sim \mathcal{U}\{1, \dots, m\}$ . Let us define:

$$(2.1) \quad \tau_i^k := \max\{\tau : \tau \leq k, i_\tau = i\},$$

i.e.,  $\tau_i^k$  is the iteration index where the  $i$ th component function is last accessed after the completion of the  $k$ th iteration. As we focus on analyzing the worst-case performance, we assume that  $\tau_i^k \in [k - K + 1, k]$  for a constant  $K = \mathcal{O}(m)$ . For example,  $K = m$  when  $i_k$  is chosen by the cyclic rule.

**First-order Approximation.** As described in (1.2), at the  $k$ th iteration the gradient method computes the *full gradient* vector as the complete sum  $\sum_{i=1}^m \nabla f_i(\boldsymbol{\theta}^k)$ . Such vector is unavailable in the incremental setting as only the access to the  $i_k$ th function is given, a simple strategy is to replace the full gradient by:

$$(2.2) \quad \mathbf{g}_{\text{IAG}}^k := \sum_{i=1}^m \nabla f_i(\boldsymbol{\theta}^{\tau_i^k}) \approx \sum_{i=1}^m \nabla f_i(\boldsymbol{\theta}^k),$$

which can be computed recursively as:

$$(2.3) \quad \mathbf{g}_{\text{IAG}}^k = \mathbf{g}_{\text{IAG}}^{k-1} - \nabla f_{i_k}(\boldsymbol{\theta}^{\tau_{i_k}^{k-1}}) + \nabla f_{i_k}(\boldsymbol{\theta}^k).$$

In particular, the formulation in (2.2) can be used to describe the SAG and IAG methods, etc., where their only differences lie in the selection scheme for  $i_k$ ; and it is also related to other methods such as SVRG and SAGA.

Note that under the smoothness assumption on component functions, we have  $\|\nabla f_i(\boldsymbol{\theta}^{\tau_i^k}) - \nabla f_i(\boldsymbol{\theta}^k)\| = \mathcal{O}(\|\boldsymbol{\theta}^{\tau_i^k} - \boldsymbol{\theta}^k\|)$ . Furthermore, [16] shows that the gradient tracking error is bounded as:

$$(2.4) \quad \|\mathbf{g}_{\text{IAG}}^k - \sum_{i=1}^m \nabla f_i(\boldsymbol{\theta}^k)\| = \mathcal{O}(\gamma m \max_{i=1, \dots, m} \|\boldsymbol{\theta}^* - \boldsymbol{\theta}^{\tau_i^k}\|),$$

we remark that this error is the ‘variance’ in gradient estimation. Eq. (2.4) implies that the tracking error decays to zero as long as  $\boldsymbol{\theta}^k$  converges to  $\boldsymbol{\theta}^*$  [recall that  $\tau_i^k - k \leq K < \infty$  and  $K = \mathcal{O}(m)$ ]. However, the dependency on  $m$  of the right hand side in (2.4) is undesirable as it leads to the following estimates:

$$(2.5) \quad \|\boldsymbol{\theta}^{k+1} - \boldsymbol{\theta}^*\|^2 \leq (1 - \mathcal{O}(\frac{\gamma}{\kappa(F)})) \|\boldsymbol{\theta}^k - \boldsymbol{\theta}^*\|^2 + \mathcal{O}(\gamma^2 m^2 \max_{(k-2K)_{++} \leq \ell \leq k} \|\boldsymbol{\theta}^\ell - \boldsymbol{\theta}^*\|^2),$$

where  $(x)_{++} := \max\{1, x\}$ . As analyzed in [16, 12], due to the dependence of  $m^2$  on the right hand side, the sequence of squared norm  $\{\|\boldsymbol{\theta}^k - \boldsymbol{\theta}^*\|^2\}_{k \geq 1}$  converges only when  $\gamma = \mathcal{O}(1/m)$ , and finally this shows that  $\|\boldsymbol{\theta}^k - \boldsymbol{\theta}^*\|^2$  converges linearly at rate  $1 - \mathcal{O}(1/(m^2 \kappa(F)))$ . Notice that a recent work [29] has strengthened this rate to  $1 - \mathcal{O}(1/(m \kappa(F)))$  and it is possible to further improve the rate through studying the expected convergence when the component function selection is random, e.g., [27].

**Second-order Approximation.** A first order approximation was applied in (2.2) to estimate the full gradient. To improve the approximation, one can consider the following Taylor expansion applied on the  $i$ th *gradient* vector itself:

$$(2.6) \quad \nabla f_i(\boldsymbol{\theta}^k) \approx \nabla f_i(\boldsymbol{\theta}^{\tau_i^k}) + \nabla^2 f_i(\boldsymbol{\theta}^{\tau_i^k})(\boldsymbol{\theta}^k - \boldsymbol{\theta}^{\tau_i^k}).$$

The right hand side gives a *second-order approximation* to the gradient of the component function  $f_i(\boldsymbol{\theta})$  evaluated at  $\boldsymbol{\theta}^k$ . Note that the approximation on the right hand side does not require access to the  $i$ th function evaluated at the current iterate  $\boldsymbol{\theta}^k$ .

Under the assumption that the Hessian of  $f_i$  is Lipschitz continuous, the Taylor approximation in (2.6) has the following error:

LEMMA 2.1. [23, Lemma 1.2.5] Assume that  $\nabla^2 f_i(\boldsymbol{\theta})$  is  $L_{H,i}$  Lipschitz. Then:

$$(2.7) \quad \left\| \nabla f_i(\boldsymbol{\theta}) - (\nabla f_i(\boldsymbol{\theta}') + \nabla^2 f_i(\boldsymbol{\theta}')(\boldsymbol{\theta} - \boldsymbol{\theta}')) \right\| \leq \frac{L_{H,i}}{2} \|\boldsymbol{\theta} - \boldsymbol{\theta}'\|^2, \quad \forall \boldsymbol{\theta}, \boldsymbol{\theta}' \in \mathbb{R}^d.$$

From Lemma 2.1, we notice that the approximation error of the right hand side in (2.6) depends on the *squared difference* between  $\boldsymbol{\theta}^k$  and  $\boldsymbol{\theta}^{\tau_i^k}$ . When  $\boldsymbol{\theta}^k$  is close to  $\boldsymbol{\theta}^{\tau_i^k}$ , this error will be significantly smaller than what is obtained for the first order approximation methods in (2.2). As a consequence, we expect an incremental method built upon the approximation (2.6) to be much faster than existing methods.

**3. Proposed Methods.** In this section, we propose two incremental methods, CIAG and A-CIAG methods, which are built from the aforementioned curvature-aided gradient tracking technique. We also comment on the implementation details such as computation and storage complexities of the proposed methods.

We develop the CIAG and A-CIAG methods from the exact full gradient (FG) and accelerated full gradient (AFG) methods, respectively. The first method, curvature-aided incremental aggregated gradient (CIAG) method, follows the recursion:

$$(3.1) \quad \boldsymbol{\theta}^{k+1} = \boldsymbol{\theta}^k - \gamma \mathbf{g}_{\text{CIAG}}^k,$$

where  $\gamma > 0$  is a step size and the gradient surrogate is

$$(3.2) \quad \mathbf{g}_{\text{CIAG}}^k := \sum_{i=1}^m (\nabla f_i(\boldsymbol{\theta}^{\tau_i^k}) - \nabla^2 f_i(\boldsymbol{\theta}^{\tau_i^k}) \boldsymbol{\theta}^{\tau_i^k}) + \left( \sum_{i=1}^m \nabla^2 f_i(\boldsymbol{\theta}^{\tau_i^k}) \right) \boldsymbol{\theta}^k,$$

where  $\tau_i^k$  was defined in (2.1). The method can be interpreted as applying the curvature-aided gradient tracking [cf. (2.6)] to *each* individual component function and following the FG update (1.2). On the other hand, the accelerated CIAG (A-CIAG) method follows the accelerated gradient (AFG) method [23] and is given by:

$$(3.3a) \quad \boldsymbol{\theta}_{ex}^k = \boldsymbol{\theta}^k + \alpha(\boldsymbol{\theta}^k - \boldsymbol{\theta}^{k-1}),$$

$$(3.3b) \quad \boldsymbol{\theta}^{k+1} = \boldsymbol{\theta}_{ex}^k - \gamma \mathbf{g}_{\text{ACIAG}}^k,$$

where  $\alpha \in [0, 1), \gamma > 0$  are predefined parameters and the gradient surrogate is

$$(3.4) \quad \mathbf{g}_{\text{ACIAG}}^k := \sum_{i=1}^m (\nabla f_i(\boldsymbol{\theta}_{ex}^{\tau_i^k}) - \nabla^2 f_i(\boldsymbol{\theta}_{ex}^{\tau_i^k}) \boldsymbol{\theta}_{ex}^{\tau_i^k}) + \left( \sum_{i=1}^m \nabla^2 f_i(\boldsymbol{\theta}_{ex}^{\tau_i^k}) \right) \boldsymbol{\theta}_{ex}^k,$$

where  $\tau_i^k$  was defined in (2.1). The term  $\boldsymbol{\theta}_{ex}^k$  in (3.3a) is called the extrapolated iterate, which incorporates the ‘inertia’ from previous iterates into the updates. Similar to the CIAG method, the A-CIAG method applies curvature-aided gradient tracking to the gradient of each individual component function, evaluated at  $\boldsymbol{\theta}_{ex}^k$ . We remark that even though Hessians are used in the CIAG and A-CIAG methods, we do not attempt to compute any matrix inverses as in the Newton methods such as NIM [26]. The Hessians here are used merely for tracking the gradients.

The CIAG and A-CIAG methods are similar in the sense that the full gradients evaluated at  $\boldsymbol{\theta}^k$  and  $\boldsymbol{\theta}_{ex}^k$  are approximated by their respective curvature-aided gradient tracking approximates [cf. (3.2) & (3.4)]. Furthermore, both methods can be implemented in a memory efficient incremental fashion. To see this, let us define

$$(3.5) \quad \boldsymbol{\theta}_i^k := \begin{cases} \boldsymbol{\theta}^{\tau_i^k}, & \text{for CIAG} \\ \boldsymbol{\theta}_{ex}^{\tau_i^k}, & \text{for A-CIAG} \end{cases},$$

**Algorithm 3.1** CIAG and A-CIAG Method.

1: **Input:** Initial point  $\boldsymbol{\theta}^1 \in \mathbb{R}^d$ , step size parameter  $\gamma > 0$ , (for A-CIAG only) extrapolation constant  $\alpha$ .

2: Initialize the vectors/matrices in the memory:

$$(3.7) \quad \boldsymbol{\theta}_i^1 = \boldsymbol{\theta}^1, \tau_i^1 = 0, \forall i, \mathbf{b}^0 = \mathbf{0}, \mathbf{H}^0 = \mathbf{0}.$$

3: **for**  $k = 1, 2, \dots$  **do**

4: Select  $i_k \in \{1, \dots, m\}$ , e.g.,  $i_k = (k \bmod m) + 1$ , and the algorithm is given access to  $f_{i_k}(\boldsymbol{\theta})$ . Set the counter variables as  $\tau_{i_k}^k = k$ ,  $\tau_j^k = \tau_j^{k-1}$  for all  $j \neq i_k$ .

5: (For A-CIAG only) If  $k = 1$ , we take  $\boldsymbol{\theta}_{ex}^1 = \boldsymbol{\theta}^1$ ; otherwise we compute the extrapolated variable as  $\boldsymbol{\theta}_{ex}^k = \boldsymbol{\theta}^k + \alpha(\boldsymbol{\theta}^k - \boldsymbol{\theta}^{k-1})$ .

6: Update the vector in the memory:

$$(3.8) \quad \boldsymbol{\theta}_{i_k}^k = \begin{cases} \boldsymbol{\theta}^k, & \text{for CIAG} , \\ \boldsymbol{\theta}_{ex}^k, & \text{for A-CIAG} , \end{cases}$$

and set  $\boldsymbol{\theta}_j^k = \boldsymbol{\theta}_j^{k-1}$  for all  $j \neq i_k$ .

7: If  $\tau_{i_k}^{k-1} = 0$ , then update: (*self-initialization*)

$$(3.9) \quad \begin{aligned} \mathbf{b}^k &= \mathbf{b}^{k-1} + \nabla f_{i_k}(\boldsymbol{\theta}_{i_k}^k) - \nabla^2 f_{i_k}(\boldsymbol{\theta}_{i_k}^k) \boldsymbol{\theta}_{i_k}^k , \\ \mathbf{H}^k &= \mathbf{H}^{k-1} + \nabla^2 f_{i_k}(\boldsymbol{\theta}_{i_k}^k) . \end{aligned}$$

Otherwise, update:

$$(3.10) \quad \begin{aligned} \mathbf{b}^k &= \mathbf{b}^{k-1} - \nabla f_{i_k}(\boldsymbol{\theta}_{i_k}^{k-1}) + \nabla f_{i_k}(\boldsymbol{\theta}_{i_k}^k) + \nabla^2 f_{i_k}(\boldsymbol{\theta}_{i_k}^{k-1}) \boldsymbol{\theta}_{i_k}^{k-1} - \nabla^2 f_{i_k}(\boldsymbol{\theta}_{i_k}^k) \boldsymbol{\theta}_{i_k}^k , \\ \mathbf{H}^k &= \mathbf{H}^{k-1} - \nabla^2 f_{i_k}(\boldsymbol{\theta}_{i_k}^{k-1}) + \nabla^2 f_{i_k}(\boldsymbol{\theta}_{i_k}^k) . \end{aligned}$$

8: Compute the update:

$$(3.11) \quad \boldsymbol{\theta}^{k+1} = \boldsymbol{\theta}_{i_k}^k - \gamma(\mathbf{b}^k + \mathbf{H}^k \boldsymbol{\theta}_{i_k}^k) .$$

9: **end for**

10: **Return:** an approximate solution to (1.1),  $\boldsymbol{\theta}^{k+1}$ .

and

$$(3.6) \quad \mathbf{b}^k := \sum_{i=1}^m (\nabla f_i(\boldsymbol{\theta}_i^k) - \nabla^2 f_i(\boldsymbol{\theta}_i^k) \boldsymbol{\theta}_i^k), \quad \mathbf{H}^k := \sum_{i=1}^m \nabla^2 f_i(\boldsymbol{\theta}_i^k) .$$

Note that  $\mathbf{b}^k$  and  $\mathbf{H}^k$  are simply the accumulation of staled iterates, gradients and Hessians. These can be computed incrementally through storing the staled iterates in memory. Moreover, we can compute the gradient surrogates as  $\mathbf{g}_{\text{CIAG}}^k = \mathbf{b}^k + \mathbf{H}^k \boldsymbol{\theta}^k$  and  $\mathbf{g}_{\text{ACIAG}}^k = \mathbf{b}^k + \mathbf{H}^k \boldsymbol{\theta}_{ex}^k$ . A pseudo code for implementing CIAG and A-CIAG is provided in Algorithm 3.1.

**3.1. Computation and Storage Costs.** We comment on the computation and storage costs of CIAG and A-CIAG. Note that (3.9), (3.10) and (3.11) in the algorithm require  $\mathcal{O}(d^2)$  FLOPS and they are the dominant computation steps involved. The overall complexities for CIAG and A-CIAG are thus  $\mathcal{O}(d^2)$  FLOPS per iteration. On the other hand, the algorithm requires storing  $m$  of  $d$ -dimensional vectors and a  $d \times d$  matrix [cf. (3.7)], therefore the storage cost is  $\mathcal{O}(md + d^2) = \mathcal{O}(md)$  if  $m \geq d$ . When  $d$  is small, the computation and storage cost of CIAG and A-CIAG are comparable to that of existing methods such as SAG, SAGA, SVRG; meanwhile for extremely large  $d$  (e.g.,  $d \geq 10^4$ ), the computation cost will be undesirable for CIAG and A-CIAG.

When the component functions are the negative log-likelihood of a linear model, the storage complexity can be reduced to as low as  $\mathcal{O}(m)$ . Note that linear models are common in learning problems such as logistic regression. In this case, we write

$$(3.12) \quad f_i(\boldsymbol{\theta}) = g_i(\langle \boldsymbol{\theta}, \mathbf{x}_i \rangle) + \frac{\rho}{2} \|\boldsymbol{\theta}\|^2,$$

where  $\mathbf{x}_i$  represents the  $i$ th associated data, while  $g_i : \mathbb{R} \rightarrow \mathbb{R}$  is twice differentiable. Observe that

$$(3.13) \quad \nabla f_i(\boldsymbol{\theta}) = g'_i(\langle \boldsymbol{\theta}, \mathbf{x}_i \rangle) \mathbf{x}_i + \rho \boldsymbol{\theta}, \quad \nabla^2 f_i(\boldsymbol{\theta}) = g''_i(\langle \boldsymbol{\theta}, \mathbf{x}_i \rangle) \mathbf{x}_i \mathbf{x}_i^\top + \rho \mathbf{I}.$$

Substituting the above into (3.10) gives:

$$(3.14) \quad \begin{aligned} \mathbf{b}^k &= \mathbf{b}^{k-1} + (g'_{i_k}(\langle \boldsymbol{\theta}_{i_k}^k, \mathbf{x}_{i_k} \rangle) - g'_{i_k}(\langle \boldsymbol{\theta}_{i_k}^{k-1}, \mathbf{x}_{i_k} \rangle)) \mathbf{x}_{i_k} \\ &\quad + \left( g''_{i_k}(\langle \boldsymbol{\theta}_{i_k}^{k-1}, \mathbf{x}_{i_k} \rangle) \langle \boldsymbol{\theta}_{i_k}^{k-1}, \mathbf{x}_{i_k} \rangle - g''_{i_k}(\langle \boldsymbol{\theta}_{i_k}^k, \mathbf{x}_{i_k} \rangle) \langle \boldsymbol{\theta}_{i_k}^k, \mathbf{x}_{i_k} \rangle \right) \mathbf{x}_{i_k} \\ \mathbf{H}^k &= \mathbf{H}^{k-1} + (g''_{i_k}(\langle \boldsymbol{\theta}_{i_k}^k, \mathbf{x}_{i_k} \rangle) - g''_{i_k}(\langle \boldsymbol{\theta}_{i_k}^{k-1}, \mathbf{x}_{i_k} \rangle)) \mathbf{x}_{i_k} \mathbf{x}_{i_k}^\top, \end{aligned}$$

and Eq. (3.9) can be simplified similarly. The above shows that it suffices for CIAG and A-CIAG to keep the inner products  $\{\langle \mathbf{x}_i, \boldsymbol{\theta}_i \rangle\}_{i=1}^m$  in order to implement the incremental updates, leading to an  $\mathcal{O}(m)$  storage cost. This observation can also be applied to the other incremental methods surveyed, e.g., SAG, SAGA, NIM, etc., except for IQN which requires storing the quasi-Hessians at the total cost of  $\mathcal{O}(md^2)$ .

**4. Convergence Analysis.** This section presents the main result of this paper regarding the convergence of CIAG and A-CIAG. In particular, we demonstrate that the proposed methods converge globally and characterize their asymptotic convergence rates. To prepare ourselves for the analysis, let us state the following assumptions.

ASSUMPTION 4.1. *The delayed iteration indices  $\tau_i^k$  [cf. (2.1)] satisfy  $0 \leq k - \tau_i^k \leq K$  for all  $i, k$ .*

ASSUMPTION 4.2.  *$F(\boldsymbol{\theta})$  is  $\mu$ -strongly convex and  $L$ -smooth with  $L \geq \mu > 0$ .*

ASSUMPTION 4.3. *Each  $f_i(\boldsymbol{\theta})$  has an  $L_{H,i}$ -Lipschitz continuous Hessian.*

We also define  $L_H := \sum_{i=1}^m L_{H,i}$  as the Lipschitz constant for the Hessian of the sum function  $F(\boldsymbol{\theta})$ . In the above, the first assumption can be satisfied when Line 4 of Algorithm 3.1 is implemented with either cyclic function selection, i.e.,  $i_k = (k \bmod m) + 1$ , or a random shuffling at the beginning of every epoch [15]. The second and the last assumptions are standard and they can be satisfied by a number of functions relevant to machine learning applications, e.g., the logistic loss function.

Let us first present the convergence result for the CIAG method — taking the parameterization  $\gamma = c/(\mu + L)$  for some  $0 < c \leq 2$ . We have:

THEOREM 4.4. *Let Assumptions 4.1, 4.2 and 4.3 hold. Consider the CIAG method with its optimality gap sequence defined as  $V^{(k)} := \|\boldsymbol{\theta}^k - \boldsymbol{\theta}^*\|^2$  where  $\boldsymbol{\theta}^*$  is the optimal solution to (1.1). If the step size parameter,  $c$ , satisfies:*

$$(4.1) \quad c < \min \left\{ 2, \frac{1}{K} \sqrt{\frac{\mu L(\mu + L)}{2L_H(L^2(V^{(1)})^{\frac{1}{2}} + 4L_H^2(V^{(1)})^{\frac{3}{2}})}}, \left( \frac{1}{K^4} \frac{\mu L(\mu + L)^4}{2L_H^2(L^4 V^{(1)} + 16L_H^4(V^{(1)})^3)} \right)^{1/5} \right\},$$

*then there exists  $\delta \in (0, 1)$  such that the sequence  $\{V^{(k)}\}_{k \geq 1}$  converges linearly, i.e.,*

$$(4.2) \quad V^{(k)} \leq \delta^{\lceil (k-1)/(2K+1) \rceil} V^{(1)}, \quad \forall k \geq 1.$$

*Moreover, there exists an upper bound sequence  $\{\bar{V}^{(k)}\}_{k \geq 1}$  — satisfying  $\bar{V}^{(k)} \geq V^{(k)}$  for all  $k \geq 1$  and  $\bar{V}^{(1)} = V^{(1)}$  such that*

$$(4.3) \quad \lim_{k \rightarrow \infty} \frac{\bar{V}^{(k+1)}}{\bar{V}^{(k)}} \leq 1 - 2\gamma \frac{\mu L}{L + \mu} = 1 - 2c \frac{\kappa(F)}{(\kappa(F) + 1)^2} = 1 - \mathcal{O}\left(\frac{c}{\kappa(F)}\right).$$

Next, for the A-CIAG method, we adopt the following parameterizations:

$$(4.4) \quad \alpha = \frac{1 - \sqrt{\mu\gamma}}{1 + \sqrt{\mu\gamma}}, \quad \gamma = \frac{c}{L},$$

for some  $0 < c \leq 1/2$ . Our convergence result is summarized below:

**THEOREM 4.5.** *Let Assumptions 4.1, 4.2 and 4.3 hold. Consider the A-CIAG method with its optimality gap sequence defined as  $h^{(k)} := F(\theta^k) - F(\theta^*)$ . If the step size parameter,  $c$ , satisfies:*

$$(4.5) \quad c < \min \{\bar{c}_1, \bar{c}_2, \bar{c}_3, 1/2\},$$

where

$$(4.6) \quad \begin{aligned} \bar{c}_1 &:= \left( \frac{\sqrt{\mu}}{\sqrt{18}K^2L_H} \frac{L^2}{\frac{20L^2}{\mu}(2h^{(1)})^{\frac{1}{2}} + \left(\frac{40L_H}{\mu}\right)^2(2h^{(1)})^{\frac{3}{2}}} \right)^{\frac{1}{2}}, \\ \bar{c}_2 &:= \left( \frac{2\mu}{81K^4L_H^2} \frac{L^4}{\left(\frac{20L^2}{\mu}\right)^2(2\bar{h}^{(1)}) + \left(\frac{40L_H}{\mu}\right)^4(2h^{(1)})^3} \right)^{\frac{1}{4}}, \\ \bar{c}_3 &:= \frac{L}{\sqrt{324}K^2L_H \frac{(h^{(1)})^{\frac{1}{2}}}{\sqrt{\mu}} + 1296K^4L_H^2 \frac{h^{(1)}}{\mu^2} + \mu}, \end{aligned}$$

then the optimality gap  $h^{(k)}$  satisfies

$$(4.7) \quad h^{(k)} \leq \delta^k(2h^{(1)}), \quad \forall k \geq 1,$$

for some  $\delta < 1$ ; moreover, there exists an upper bound sequence  $\{\bar{h}^{(k)}\}_{k \geq 1}$  such that  $\bar{h}^{(k)} \geq h^{(k)}$  for all  $k \geq 1$  and  $\bar{h}^{(1)} = h^{(1)}$ , such that

$$(4.8) \quad \lim_{k \rightarrow \infty} \frac{\bar{h}^{(k+1)}}{\bar{h}^{(k)}} = 1 - \sqrt{\mu\gamma} = 1 - \sqrt{\frac{c}{\kappa(F)}}.$$

The above theorems reveal that there are two phases of convergence for the CIAG and A-CIAG methods – one that converges at a *slow* linear rate [cf. (4.2) and (4.7)], and the asymptotic phase where the algorithms converge linearly at a *fast* rate comparable to the FG and AFG methods [cf. (4.3) and (4.8)]. Such behavior is similar to the linear and superlinear convergence phases in the Newton's method [5], and they can be anticipated as the CIAG and A-CIAG methods make use of the second order information.

Notice that due to the strong convexity of  $F(\theta)$  [cf. Assumption 4.2], the Lyapunov function used in the two theorems above are comparable, since

$$(4.9) \quad \frac{\mu}{2}V^{(k)} \leq h^{(k)} \leq \frac{L}{2}V^{(k)} \implies h^{(k)} = \Theta(V^{(k)}).$$

Moreover, both theorems require the step size parameters be chosen according to the initial conditions [cf. (4.1) and (4.5)]. The allowable range of step size  $\gamma$  is inversely proportional to  $L_H$  and  $V^{(1)}$ . Here, the former term  $L_H$  measures the ‘quadratic-ness’ of the component functions such that  $L_H = 0$  if  $f_i(\theta)$  are quadratic. The latter term  $V^{(1)}$  is the initial optimality gap for the algorithm. The favorable cases are when  $L_H \approx 0$  or  $V^{(1)} \approx 0$  such that we can take  $c = \Theta(1)$ . The latter implies the following asymptotic convergence rates:

$$(4.10) \quad \text{CIAG : } \lim_{k \rightarrow \infty} \frac{\bar{V}^{(k+1)}}{\bar{V}^{(k)}} = 1 - \mathcal{O}\left(\frac{1}{\kappa(F)}\right), \quad \text{A-CIAG : } \lim_{k \rightarrow \infty} \frac{\bar{h}^{(k+1)}}{\bar{h}^{(k)}} = 1 - \sqrt{\frac{1/2}{\kappa(F)}},$$

*i.e.*, they coincide with the convergence rates achieved by the FG and AFG methods, respectively. Since the per-iteration complexity of CIAG and A-CIAG are  $\mathcal{O}(d^2)$ , while the complexity of FG and AFG are  $\mathcal{O}(md)$ , the advantage of the proposed methods is significant when  $m \gg d$ .

It is also interesting to compare the convergence results for the CIAG and A-CIAG methods. From the outset, most noticeably, the A-CIAG criterion (4.6) differs from the CIAG criterion (4.1) for the region specified by  $\tilde{c}_3$  as the latter requires the step size parameter be chosen as  $c = \mathcal{O}(1/K^4)$  for large  $K$ . Since  $K = \Theta(m)$ , this implies that the initial optimality gap has to be as small as  $h^{(1)} = \mathcal{O}(1/m^4)$  to attain the fastest convergence rate in (4.10). In comparison, the CIAG method only requires  $V^{(1)} = \mathcal{O}(1/m)$  to attain (4.10) due to the milder requirements in (4.1). Nevertheless, we remark that these criterion analyzes the worst case scenario and the practical step sizes can be chosen more aggressively. As we shall demonstrate in Section 5, both CIAG and A-CIAG methods exhibit fast convergence with a far larger step size than the one predicted by the theorems.

**4.1. Proofs of Theorem 4.4 and 4.5.** The convergence analysis for both CIAG and A-CIAG methods consists of the following three steps.

- First, we carry out a perturbation analysis on the FG and AFG methods. This is motivated by viewing the CIAG (*resp.* A-CIAG) method as a perturbed FG (*resp.* AFG) method with inexact gradient resulted from curvature-aided gradient tracking. Specifically, the gradient errors involved are defined as:

$$(4.11) \quad \mathbf{e}_{\text{CIAG}}^k := \mathbf{g}_{\text{CIAG}}^k - \sum_{i=1}^m \nabla f_i(\boldsymbol{\theta}^k), \quad \mathbf{e}_{\text{ACIAG}}^k := \mathbf{g}_{\text{ACIAG}}^k - \sum_{i=1}^m \nabla f_i(\boldsymbol{\theta}_{ex}^k).$$

Note that at this stage, we did not exploit the structure of the gradient error and the analysis result can be applied to any perturbed gradient methods.

- Second, we analyze an upper bound on  $\|\mathbf{e}_{\text{CIAG}}^k\|$  or  $\|\mathbf{e}_{\text{ACIAG}}^k\|$  in terms of the optimality gaps

$$(4.12) \quad V^{(k)} := \|\boldsymbol{\theta}^k - \boldsymbol{\theta}^*\|^2, \quad h^{(k)} := F(\boldsymbol{\theta}^k) - F(\boldsymbol{\theta}^*),$$

where we shall use  $V^{(k)}$ ,  $h^{(k)}$  as the Lyapunov functions for CIAG method and A-CIAG method, respectively. Here, we have exploited Assumption 4.3 on the Lipschitz continuity of Hessian for the component functions.

- Third, using the bounds derived in the previous steps we study a nonlinear inequality system to derive the convergence criterion of  $V^{(k)}$  and  $h^{(k)}$ . The nonlinear inequality exhibits the desired convergence rates when  $k \rightarrow \infty$ .

Overall, the key to our proof is to analyze the dynamics of optimality gap  $V^{(k)}$  (or  $h^{(k)}$ ) as a nonlinear system, whose convergence can be guaranteed by an appropriately chosen step size  $\gamma$  and the asymptotic convergence rate will only depend on the linear terms in the optimality gaps.

In the following analysis, we assume that the CIAG and ACIAG methods are both initialized such that (3.6) holds. This can be done ‘on-the-fly’ using the self-initialization step in (3.9) and the analysis below will hold for all  $k \geq K$ , *i.e.*, after a complete pass through the dataset.

**Step 1.** The first step is to analyze the CIAG (*resp.* A-CIAG) method as a perturbed version of the FG (*resp.* AFG) method, which employs  $\mathbf{g}_{\text{CIAG}}^k$  (*resp.*  $\mathbf{g}_{\text{ACIAG}}^k$ ) as the gradient surrogate. We have the following propositions:

**PROPOSITION 4.6.** *Consider the CIAG method. Under Assumption 4.2, if  $\gamma \leq 2/(\mu + L)$ , we have that for all  $k \geq 1$ ,*

$$(4.13) \quad V^{(k+1)} \leq \left(1 - 2\gamma \frac{\mu L}{\mu + L}\right) V^{(k)} + \gamma^2 \|\mathbf{e}_{\text{CIAG}}^k\|^2 + 2\gamma \sqrt{V^{(k)}} \|\mathbf{e}_{\text{CIAG}}^k\|.$$

PROPOSITION 4.7. *Consider the A-CIAG method. Under Assumption 4.2, if  $\gamma \leq 1/(2L)$ , we have that for all  $k \geq 1$ ,*

$$(4.14) \quad \begin{aligned} h^{(k+1)} &\leq 2(1 - \sqrt{\mu\gamma})^k h^{(1)} + \sum_{\ell=1}^k (1 - \sqrt{\mu\gamma})^{k-\ell} \left( \sqrt{2\gamma h^{(\ell)}} \|e_{\text{ACIAG}}^\ell\| \right. \\ &\quad \left. + \sqrt{\frac{9\gamma}{\mu}} \|e_{\text{ACIAG}}^\ell\|^2 - \frac{\mu}{4} \frac{1 - \mu\gamma}{\sqrt{\mu\gamma}} \|\theta^\ell - \theta_{ex}^\ell\|^2 \right). \end{aligned}$$

From the propositions, we observe that when the gradient errors vanish with  $e^\ell = \mathbf{0}$ , setting  $\gamma = 2/(\mu + L)$  (resp.  $\gamma = 1/(2L)$ ) gives  $V^{(k+1)} = \mathcal{O}((1 - 1/\kappa(F))^k)$  (resp.  $h^{(k+1)} = \mathcal{O}((1 - \sqrt{1/2\kappa(F)})^k)$ ). In other words, the linear convergence rates for FG and AFG methods can be recovered.

Comparing the two propositions reveals the differences in error structure for the CIAG and A-CIAG methods — first, in (4.14) the A-CIAG's error is convolved with the linearly converging sequence  $(1 - \sqrt{\mu\gamma})^\ell$ , while in (4.13) the CIAG's error is simply additive; second, (4.14) consists of a negative term depending on  $\|\theta^\ell - \theta_{ex}^\ell\|^2$ . These differences will be accounted for when analyzing convergence in the forthcoming steps.

**Step 2.** Our next step is to relate the gradient errors  $e_{\text{CIAG}}^\ell \neq \mathbf{0}$ ,  $e_{\text{ACIAG}}^\ell \neq \mathbf{0}$  to the optimality gaps  $V^{(\ell)}$ ,  $h^{(\ell)}$  for the CIAG, A-CIAG methods, respectively. We obtain bounds for errors in the curvature-aided gradient surrogates as follows:

PROPOSITION 4.8. *Consider the CIAG method. Under Assumptions 4.1, 4.2 and 4.3, we have that for all  $\ell \geq 1$ ,*

$$(4.15) \quad \|e_{\text{CIAG}}^\ell\| \leq \gamma^2 K^2 L_H \left( L^2 \max_{(\ell-K)_{++} \leq q \leq \ell-1} V^{(q)} + 4L_H^2 \max_{(\ell-2K)_{++} \leq q \leq \ell-1} (V^{(q)})^2 \right).$$

PROPOSITION 4.9. *Consider the A-CIAG method. Under Assumptions 4.1, 4.2 and 4.3, we have that for all  $\ell \geq 1$ ,*

$$(4.16) \quad \begin{aligned} \|e_{\text{ACIAG}}^\ell\| &\leq \frac{3KL_H}{2} \sum_{j=(\ell-K)_{++}}^{\ell-1} \|\theta^{j+1} - \theta_{ex}^{j+1}\|^2 + \gamma^2 \frac{3K^2 L_H}{2} \frac{20L^2}{\mu} \max_{(\ell-K-1)_{++} \leq q \leq \ell-1} h^{(q)} \\ &\quad + \gamma^2 \frac{3K^2 L_H}{2} \left( \frac{40L_H}{\mu} \right)^2 \max_{(\ell-2K-1)_{++} \leq q \leq \ell-1} (h^{(q)})^2. \end{aligned}$$

We see that if  $L_H = 0$ , i.e.,  $f_i(\theta)$  are quadratic, then  $e_{\text{CIAG}}^\ell = e_{\text{ACIAG}}^\ell = \mathbf{0}$  for all  $\ell \geq 1$ .

We observe that the upper bounds for  $\|e_{\text{CIAG}}^k\|$  and  $\|e_{\text{ACIAG}}^k\|$  obey similar structure in terms of their dependences on  $V^{(q)}$  and  $h^{(q)}$ . In addition, the upper bound for  $\|e_{\text{ACIAG}}^\ell\|$  depends on  $\{\|\theta^{j+1} - \theta_{ex}^{j+1}\|^2\}_{j=(\ell-K)_{++}}^{\ell-1}$  which is the difference between the extrapolated variables and the main variables. As seen in the next step, this additional error leads to a smaller region of convergence for the A-CIAG method.

**Step 3.** To keep the notations simple, in the following discussions we omit the detailed constants which are obtained from the propositions given in the previous steps. Instead, we focus on the main steps in the analysis and relegate the exact analysis to Appendices C and G.

For the CIAG method, we observe that incorporating (4.15) into the right hand side of (4.13) yields:

$$(4.17) \quad \begin{aligned} V^{(k+1)} &\leq \left( 1 - 2\gamma \frac{\mu L}{\mu + L} \right) V^{(k)} \\ &\quad + \mathcal{O}(\gamma^3) \max_{(k-2K)_{++} \leq q \leq k} \left( (V^{(q)})^{\frac{3}{2}} + (V^{(q)})^2 + (V^{(q)})^{\frac{5}{2}} + (V^{(q)})^4 \right), \end{aligned}$$

where the exact form of the system will be shown in (C.1). Define that

$$(4.18) \quad V_{\max}^{(k)} := \max_{(k-2K)_{++} \leq q \leq k} V^{(q)}$$

and using the fact that, when  $V^{(k)}$  is small, the second part in the right hand side of (4.17) can be bounded by its lowest order term  $\mathcal{O}(\gamma^3)(V_{\max}^{(k)})^{\frac{3}{2}}$ , we thus have:

$$(4.19) \quad V^{(k+1)} \leq \left(1 - 2\gamma \frac{\mu L}{\mu + L}\right) V^{(k)} + \mathcal{O}(\gamma^3)(V_{\max}^{(k)})^{\frac{3}{2}}.$$

On the other hand, for the A-CIAG method, incorporating the right hand side of (4.16) into (4.14) and rearranging terms show that the  $(k+1)$ th optimality gap is bounded as follows:

$$(4.20) \quad \begin{aligned} h^{(k+1)} &\leq 2(1 - \sqrt{\mu\gamma})^k h^{(1)} + \sum_{\ell=1}^k (1 - \sqrt{\mu\gamma})^{k-\ell} \\ &\quad \left( \mathcal{O}(\gamma^{\frac{5}{2}}) \max_{(\ell-2K-1)_{++} \leq q \leq \ell} ((h^{(q)})^{\frac{3}{2}} + (h^{(q)})^2 + (h^{(q)})^{\frac{5}{2}} + (h^{(q)})^4) + \right. \\ &\quad \left. \left( \max_{\ell \leq q \leq \min\{\ell+K, k\}} \mathcal{O}(\sqrt{\gamma h^{(q)}}) - \frac{\mu}{4} \frac{1 - \mu\gamma}{\sqrt{\mu\gamma}} \right) \|\theta^\ell - \theta_{ex}^\ell\|^2 \right), \end{aligned}$$

whose exact form can be found in (G.5). We emphasize that the last term on the right hand side depends on the difference between  $\theta^\ell$  and  $\theta_{ex}^\ell$ , which is unique for A-CIAG method due to the use of extrapolated iterates.

To finish the proof, we identify that in both (4.19) and (4.20), the Lyapunov functions for CIAG and A-CIAG methods, *i.e.*,  $V^{(k+1)}$  and  $h^{(k+1)}$ , are upper bounded by — a constant factor ( $< 1$ ) multiplied by the previous Lyapunov function's value; and a *high-order* term that depends on the delayed version of the Lyapunov function's value. With a sufficiently small step size, the effects from the later term vanishes as  $k \rightarrow \infty$  and the proposed methods converge linearly at the desired rates.

Particularly, in the case of CIAG, we consider the *non-linear* inequality:

$$(4.21) \quad R^{(k+1)} \leq pR^{(k)} + \sum_{j=1}^J q_j \max_{k' \in [(k-M+1)_{++}, k]} (R^{(k')})^{\eta_j}, \quad \forall k \geq 1,$$

where  $0 \leq p < 1$ ,  $q_j \geq 0$ ,  $\eta_j > 1$  for all  $j$  with some  $J, M < \infty$ . We have:

PROPOSITION 4.10. *Consider (4.21). For some  $p \leq \delta < 1$ , if*

$$(4.22) \quad p + \sum_{j=1}^J q_j (R^{(1)})^{\eta_j - 1} \leq \delta < 1,$$

*then (a)  $\{R^{(k)}\}_{k \geq 1}$  converges linearly as  $R^{(k)} \leq \delta^{\lceil k/M \rceil} R^{(1)}$  for all  $k \geq 1$ ; (b) there exists an upper bound sequence  $\{\bar{R}^{(k)}\}_{k \geq 1}$  with  $\bar{R}^{(k)} \geq R^{(k)}$  for all  $k \geq 1$  and  $\bar{R}^{(1)} = R^{(1)}$ , that converges linearly at rate  $p$  asymptotically,*

$$(4.23) \quad \lim_{k \rightarrow \infty} \bar{R}^{(k+1)} / \bar{R}^{(k)} = p.$$

Consequently, Theorem 4.4 can be proven by identifying that  $R^{(k)} = V^{(k)}$  and substituting the appropriate constants in Proposition 4.10.

In the case of A-CIAG, it can be verified that under our choice of step size, the coefficient in front of  $\|\theta^\ell - \theta_{ex}^\ell\|^2$  is always negative for all  $\ell \geq 1$ . If we define

$$(4.24) \quad h_{\max}^{(\ell)} := \max_{(\ell-2K-1)_{++} \leq q \leq \ell} h^{(q)}.$$

When  $h_{\max}^{(\ell)}$  is small, the terms inside the last bracket of the summation in (4.20) can be bounded by its lowest order term as  $\mathcal{O}(\gamma^{\frac{5}{2}})(h_{\max}^{(\ell)})^{\frac{3}{2}}$ . Therefore, we can consider an upper bound sequence  $\{\bar{h}^{(k)}\}_{k \geq 1}$  such that  $\bar{h}^{(k)} \geq h^{(k)}$  for all  $k$  and:

$$(4.25) \quad \bar{h}^{(k+1)} = 2(1 - \sqrt{\mu\gamma})^k \bar{h}^{(1)} + \sum_{\ell=1}^k (1 - \sqrt{\mu\gamma})^{k-\ell} \mathcal{O}(\gamma^{\frac{5}{2}})(\bar{h}_{\max}^{(\ell)})^{\frac{3}{2}}.$$

Subtracting  $(1 - \sqrt{\mu\gamma})\bar{h}^{(k)}$  from both sides gives:

$$(4.26) \quad \bar{h}^{(k+1)} = (1 - \sqrt{\mu\gamma})\bar{h}^{(k)} + \mathcal{O}(\gamma^{\frac{5}{2}})(\bar{h}_{\max}^{(k)})^{\frac{3}{2}},$$

which resembles (4.19) in the case of CIAG. Similar to the previous developments, we expect the system to converge linearly at the rate  $1 - \sqrt{\mu\gamma}$ .

Formally, consider an abstraction from (4.20) with the non-negative sequence  $\{R^{(k)}\}_{k \geq 1}$  that satisfies:

$$(4.27) \quad R^{(k+1)} \leq p^k b R^{(1)} + \sum_{\ell=1}^k p^{k-\ell} \left( \sum_{j=1}^J s_j \max_{\{\ell-M\}++ \leq q \leq \ell} (R^{(q)})^{\eta_j} - (\bar{f} - \max_{\ell \leq q \leq k} f(R^{(q)})) D^{(\ell)} \right),$$

for all  $k \geq 1$ , where  $f(R^{(q)})$  is a non-decreasing function of  $R^{(q)}$  and  $\eta_j > 1$  for all  $j$ . The parameters  $p, s_j, \bar{f}, b$  are all non-negative, we have  $b \geq 1$  and  $M < \infty$ , and  $\{D^{(\ell)}\}_{\ell \geq 1}$  is an arbitrary non-negative sequence. The above system converges linearly at a rate given by the constant factor  $p < 1$ , as shown below:

PROPOSITION 4.11. *Consider (4.27). Suppose that*

$$(4.28) \quad \bar{f} \geq f(bR^{(1)}) \quad \text{and} \quad \delta := p + \sum_{j=1}^J s_j (bR^{(1)})^{\eta_j-1} < 1.$$

*Then, there exists an upper bound sequence  $\{\bar{R}^{(k)}\}_{k \geq 1}$  satisfying*

$$(4.29) \quad \begin{aligned} (i) \quad & \bar{R}^{(k)} \geq R^{(k)}, \quad \forall k \geq 1, \quad (ii) \quad \bar{R}^{(k+1)} \leq \delta^{\lceil k/M \rceil} (b\bar{R}^{(1)}), \quad \forall k \geq 1 \\ \text{and} \quad (iii) \quad & \lim_{k \rightarrow \infty} \frac{\bar{R}^{(k+1)}}{\bar{R}^{(k)}} = p. \end{aligned}$$

Finally, Theorem 4.5 can be proven by identifying  $R^{(k)} = h^{(k)}$  and substituting the appropriate constants.

**4.2. Discussion: ‘Accelerated’ IAG Method.** The accelerated rate proven in Theorem 4.5 – that is independent of the number of component functions when the initialization is sufficiently close to optimal – is achieved mainly due to the use of second-order approximation in our gradient tracking technique. To illustrate this point, in this section we provide a counter example by applying a similar analysis strategy to an ‘accelerated’ IAG method and demonstrate that its convergence is linear with a potentially worse rate than the original IAG method [7].

The ‘accelerated’ IAG method of interest can be described as:

$$(4.30) \quad \theta_{ex}^k = \theta^k + \alpha(\theta^k - \theta^{k-1}), \quad \theta^{k+1} = \theta_{ex}^k - \gamma \sum_{i=1}^m \nabla f_i(\theta_{ex}^k).$$

Similar to the A-CIAG method, we also take  $\alpha = (1 - \sqrt{\mu\gamma})/(1 + \sqrt{\mu\gamma})$  and  $\gamma \leq 1/(2L)$ . With a slight abuse of notation, we define  $\mathbf{g}^k := \sum_{i=1}^m \nabla f_i(\theta_{ex}^k)$ ,  $\mathbf{e}^k := \mathbf{g}^k - \sum_{i=1}^m \nabla f_i(\theta_{ex}^k)$ , as the gradient surrogate and error used, respectively. Once again, we can view this ‘accelerated’ IAG method as a

perturbed AFG method, whose optimality gap,  $h^{(k)} := F(\boldsymbol{\theta}^k) - F(\boldsymbol{\theta}^*)$ , follows the conclusion from Proposition 4.7:

$$(4.31) \quad \begin{aligned} h^{(k+1)} &\leq (1 - \sqrt{\mu\gamma})^k (2h^{(1)}) + \sum_{\ell=1}^k (1 - \sqrt{\mu\gamma})^{k-\ell} \left( \sqrt{2\gamma h^{(\ell)}} \|e^\ell\| \right. \\ &\quad \left. + \sqrt{\frac{9\gamma}{\mu}} \|e^\ell\|^2 - \frac{\mu}{4} \frac{1 - \mu\gamma}{\sqrt{\mu\gamma}} \|\boldsymbol{\theta}^\ell - \boldsymbol{\theta}_{ex}^\ell\|^2 \right). \end{aligned}$$

By essentially repeating the proof for Proposition 4.9, we can show:

$$(4.32) \quad \|e^\ell\| \leq L \sum_{j=(\ell-m)_{++}}^{\ell-1} \|\boldsymbol{\theta}^{j+1} - \boldsymbol{\theta}_{ex}^{j+1}\| + 8\gamma mL^2 \sqrt{\frac{2}{\mu}} \max_{(\ell-2m-1)_{++} \leq q \leq \ell} \sqrt{h^{(q)}}.$$

Substituting (4.32) into (4.31) gives:

$$\begin{aligned} h^{(k+1)} &\leq (1 - \sqrt{\mu\gamma})^k (2h^{(1)}) + \sum_{\ell=1}^k (1 - \sqrt{\mu\gamma})^{k-\ell} \left( \mathcal{O}(\gamma^{\frac{3}{2}} mL^2 / \mu^{\frac{1}{2}}) \max_{(\ell-2m-1)_{++} \leq q \leq \ell} h^{(q)} \right. \\ &\quad \left. + \underbrace{\left( \mathcal{O}(\sqrt{\gamma}) - \frac{\mu}{4} \frac{1 - \mu\gamma}{\sqrt{\mu\gamma}} \right) \|\boldsymbol{\theta}^\ell - \boldsymbol{\theta}_{ex}^\ell\|}_{\leq 0 \text{ for suff. small } \gamma} \right) \\ &\leq (1 - \sqrt{\mu\gamma})^k (2h^{(1)}) + \sum_{\ell=1}^k (1 - \sqrt{\mu\gamma})^{k-\ell} \mathcal{O}(\gamma^{\frac{3}{2}} mL^2 / \mu^{\frac{1}{2}}) \max_{(\ell-2m-1)_{++} \leq q \leq \ell} h^{(q)}. \end{aligned}$$

Consider an upper bound sequence  $\bar{h}^{(k)} \geq h^{(k)}$  such that the above inequality is tight. It can be shown that:

$$(4.33) \quad \bar{h}^{(k+1)} = (1 - \sqrt{\mu\gamma}) \bar{h}^{(k)} + \mathcal{O}(\gamma^{\frac{3}{2}} mL^2 / \mu^{\frac{1}{2}}) \max_{(k-2m-1)_{++} \leq q \leq k} \bar{h}^{(q)}.$$

Finally, Lemma 3.2 from [16] shows that the sequence  $\{\bar{h}^{(k)}\}_{k \geq 1}$  converges if  $1 - \sqrt{\mu\gamma} + \mathcal{O}(\gamma^{\frac{3}{2}} mL^2 / \mu^{\frac{1}{2}}) < 1$ , which holds if  $\gamma = \mathcal{O}(1/(mL\kappa(F)))$ . The resultant rate is:

$$(4.34) \quad \left( 1 - \mathcal{O}(1/\sqrt{m^3\kappa(F)}) \right)^{1/m} \approx 1 - \mathcal{O}(1/\sqrt{m^5\kappa(F)}).$$

For large  $m$ , the rate in (4.34) is worse than the rate of  $1 - \mathcal{O}(1/(m\kappa(F)))$  analyzed in [29] for IAG.

The analysis above shows that the theoretical convergence rate may not be improved using the acceleration technique that we have applied in A-CIAG, as long as the same analysis framework for A-CIAG was adopted. The interested readers are referred to the analysis on IAG-M, *i.e.*, IAG with momentum, in [16], which also showed a linear convergence rate without acceleration, despite that IAG-M adopted a similar acceleration technique as (4.30).

**5. Numerical Experiments.** This section covers the performance of CIAG and A-CIAG using numerical experiments. We focus on the logistic regression problem for training linear classifiers. In the following experiments, we are given  $m$  data tuples  $\{(\mathbf{x}_i, y_i)\}_{i=1}^m$ , where  $\mathbf{x}_i \in \mathbb{R}^d$  is the feature vector and  $y_i \in \{\pm 1\}$  is the label. The  $i$ th component function is:

$$(5.1) \quad f_i(\boldsymbol{\theta}) = \frac{1}{2m} \|\boldsymbol{\theta}\|^2 + \log(1 + \exp(-y_i \langle \boldsymbol{\theta}, \mathbf{x}_i \rangle)).$$

This function has the form of a linear model in (3.12) and it also satisfies Assumptions 4.2 and 4.3. For instance, an upper bound to the gradient and Hessian smoothness of  $F(\boldsymbol{\theta})$  and  $f_i(\boldsymbol{\theta})$ , respectively, can be evaluated as:

$$(5.2) \quad L = 1 + \frac{1}{4} \sum_{i=1}^m \|\mathbf{x}_i\|_2^2, \quad L_{H,i} = \frac{1}{4} \|\mathbf{x}_i\|_2^2.$$

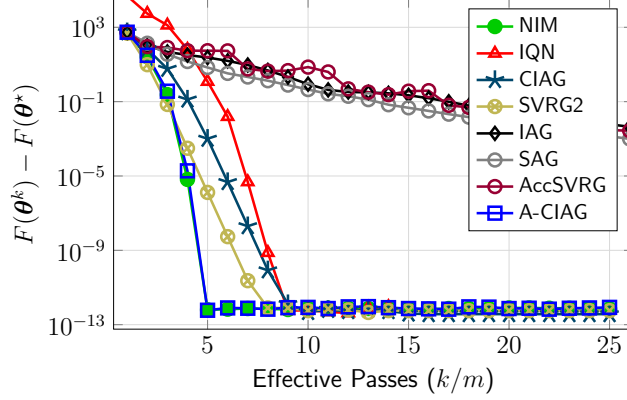


FIG. 1. Comparison on synthetic data with  $m = 1000$ ,  $d = 51$ . The y-axis denotes the optimality gap plotted in log-scale and the x-axis shows the number of effective passes (defined as  $k/m$ ). For A-CIAG, we set the extrapolation weight as  $\alpha = 0.95$ . For NIM and SVRG2, we use the step size of  $\gamma = 1$  and  $\gamma = 1/L$ , respectively. SVRG2, AccSVRG require a full gradient/Hessian evaluation step per epoch and the actual numbers of effective passes required are higher than it is shown. The x-axis does not account for these full gradient/Hessian evaluations. We scaled up the plot horizontally for AccSVRG as the latter uses a minibatch of size 5.

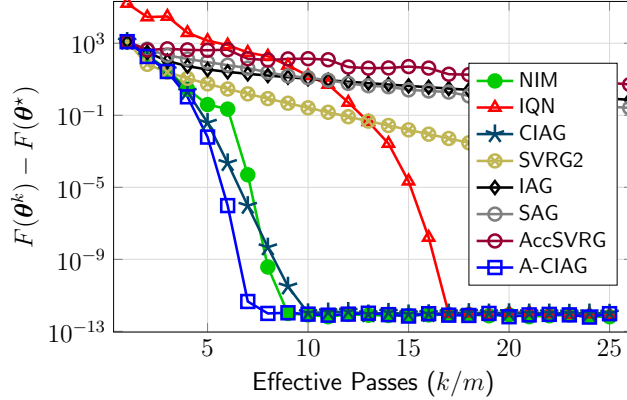


FIG. 2. Comparison on synthetic data with  $m = 2000$ ,  $d = 501$ . For A-CIAG, we set the extrapolation weight as  $\alpha = 0.6$ . For NIM and SVRG2, we use the step size of  $\gamma = 0.01$  and  $\gamma = 0.1/L$ , respectively. The x-axis does not account for the full gradient/Hessian evaluations in SVRG2 and AccSVRG at the beginning of each epoch.

**5.1. Synthetic Data.** We adopt a simple random data model. First, we generate  $\theta_{\text{true}} \sim \mathcal{U}[-1, 1]^d$  and the feature vector as  $x_i = [\tilde{x}_i; 1]$  where  $\tilde{x}_i \sim \mathcal{U}[-1, 1]^{d-1}$ ; then, the label is computed as  $y_i = \text{sign}(\langle x_i, \theta_{\text{true}} \rangle)$ .

To set up the benchmark, the step sizes for NIM and IQN are  $\gamma = 1$ . For the IAG method, we set  $\gamma = 50/(mL)$ . For the CIAG and A-CIAG methods, we set  $\gamma = 1/L$  and we specify the extrapolation weight for A-CIAG later. The above methods are implemented with deterministic, cyclic component function selection, *i.e.*,  $i_k = (k \bmod m) + 1$ . We also compare a few stochastic methods: for SAG and AccSVRG, we set  $\gamma = 50/(mL)$ ; and the batch size is  $B = 5$  for AccSVRG with an epoch length of  $m$ . For SVRG2, we set an epoch length of  $0.1m$ . The step sizes for NIM and SVRG2 will be specified later.

The evolution of the optimality gap against the number of effective passes through data are shown in Figure 1 and 2 for different problem sizes. We defined the number of effective passes as the number of iterations ( $k$ ) divided by  $m$ . From Figure 1 and 2, we observe that both NIM and IQN methods have the fastest convergence, since both methods are shown to converge superlinearly. However, we note that the curvature aided methods, A-CIAG, CIAG and SVRG2, also demonstrate similar convergence speed in terms of the number of effective data passes used. Especially, the speed of the proposed A-CIAG almost matches that of the NIM method.

Dataset	A-CIAG	CIAG	NIM	SAG <sup>‡</sup>
<b>mushrooms</b> ( $m = 8124, d = 112$ )	<b>5.22 pass</b> <b>0.299 sec.</b>	43.5 pass 2.509 sec.	4.81 (4.92) pass 1.01 (0.329) sec.	359.9 pass 1.521 sec.
<b>a9a</b> ( $m = 32561, d = 123$ )	<b>3.6 pass</b> <b>1.067 sec.</b>	52.2 pass 15.26 sec.	3.0 (3.2) pass 3.38 (1.10) sec.	165.8 pass 3.685 sec.
<b>SUSY</b> ( $m = 5 \times 10^6, d = 18$ )	<b>7.1 pass</b> <b>24.88 sec.</b>	7.6 pass 26.81 sec.	6.2 (6.2) pass 35.92 (29.82) sec.	52.3 pass 99.00 sec.
<b>covtype</b> ( $m = 581012, d = 54$ )	<b>4.5 pass</b> <b>5.888 sec.</b>	13.5 pass 17.71 sec.	4.0 (4.5) pass 13.84 (7.06) sec.	101.9 pass 32.33 sec.
<b>w8a</b> ( $m = 49749, d = 300$ )	<b>5.5 pass</b> <b>12.73 sec.</b>	7.2 pass 16.48 sec.	5.3 (5.4) pass 69.13 (13.82) sec.	251.01 pass 23.20 sec.
<b>mnist</b> ( $m = 60000, d = 784$ )	4.3 pass 89.59 sec.	143.6 pass 2801 sec.	3.8 ( <b>3.8</b> ) pass <b>755.2 (86.94) sec.</b>	$\geq 10^3$ pass $\geq 392$ sec. <sup>†</sup>
<b>alpha</b> ( $m = 5 \times 10^5, d = 500$ )	<b>2.4 pass</b> <b>149.5 sec.</b>	7.6 pass 475.6 sec.	2.3 (2.5) pass 1111.6 (176.4) sec.	80.5 pass 210.7 sec.

TABLE 2

Performance comparison on different datasets. We show the number of effective passes (defined as  $k/m$ ) and the wall clock time required to reach convergence with  $\|\nabla F(\theta^k)\| \leq 10^{-10}$ . For the NIM method, we tested both ‘exact’ and ‘inexact’ settings in the computation of Hessian inverse. The results inside the brackets (·) correspond to the ‘inexact’ setting. (<sup>†</sup> The algorithms are terminated when  $k/m \geq 10^3$  and the wall clock time is the total elapsed time at termination. <sup>‡</sup> The results for SAG are averaged over 10 trials.)

	mushrooms	a9a	SUSY	covtype	w8a	mnist	alpha
A-CIAG	$\gamma = \frac{10^{-3}}{L}$ $\alpha = 0.99$	$\gamma = \frac{10^{-4}}{L}$ $\alpha = 0.99$	$\gamma = \frac{10^{-5}}{L}$ $\alpha = 0.99$	$\gamma = \frac{5 \cdot 10^{-6}}{L}$ $\alpha = 0.99$	$\gamma = \frac{10^{-3}}{L}$ $\alpha = 0.99$	$\gamma = \frac{10^{-4}}{L}$ $\alpha = 0.99$	$\gamma = \frac{5 \cdot 10^{-6}}{L}$ $\alpha = 0.99$
CIAG	$\gamma = \frac{10^{-3}}{L}$	$\gamma = \frac{2 \cdot 10^{-4}}{L}$	$\gamma = \frac{10^{-5}}{L}$	$\gamma = \frac{5 \cdot 10^{-6}}{L}$	$\gamma = \frac{10^{-3}}{L}$	$\gamma = \frac{10^{-4}}{L}$	$\gamma = \frac{10^{-5}}{L}$
SAG	$\gamma = \frac{1}{mL}$	$\gamma = \frac{1}{mL}$	$\gamma = \frac{1}{mL}$	$\gamma = \frac{1}{mL}$	$\gamma = \frac{1}{mL}$	$\gamma = \frac{1}{mL}$	$\gamma = \frac{1}{mL}$
NIM	$\gamma = 1$	$\gamma = 1$	$\gamma = 1$	$\gamma = 1$	$\gamma = 1$	$\gamma = 1$	$\gamma = 1$

TABLE 3

Parameters used for A-CIAG, CIAG, SAG, NIM methods in the numerical experiments.

**5.2. Real Data.** We empirically compare the algorithms on the datasets from LibSVM [10]. For this example, the algorithms are implemented in C++ based on the source codes by [26] (available: [http://github.com/arodomanov/nim\\_icml16\\_code](http://github.com/arodomanov/nim_icml16_code)) to demonstrate the fastest possible practical performance. We only compare the proposed CIAG, A-CIAG to IAG, NIM and SAG, where the first four algorithms employ a deterministic, cyclic component function selection and the last algorithm employs random component function selection. For the NIM method, we tested both of its *exact* and *inexact* setting, where the *inexact* setting is a double-loop method which uses a conjugate gradient method to tackle the Hessian inverse involved. We have used a mini-batch setting for all the tested methods such that each  $f_i(\theta)$  is composed of  $B = 5$  data tuples. The numerical experiments were conducted on a Laptop computer with an Intel Core i7 2.8Ghz quad-core processor and 16 gigabytes of memory.

An overview of the performance comparison can be found in Table 2, while Table 3 shows the algorithms’ parameter settings used for different dataset. As seen, the A-CIAG method outperformed the benchmarks for many of the considered datasets in terms of the wall clock convergence time, and the number of effective passes required is comparable to the best available method, NIM. An exception is the experiment on the **mnist** dataset. We suspect that this is due to the potentially poor condition number with the **mnist** dataset, as we observe that the unaccelerated methods SAG, IAG and CIAG exhibit significantly slower convergence than for the other datasets. Nevertheless, even in this scenario A-CIAG and NIM performance are still comparable.

To investigate the behavior of the algorithms, Figure 3 shows the evolution of gradient’s norm

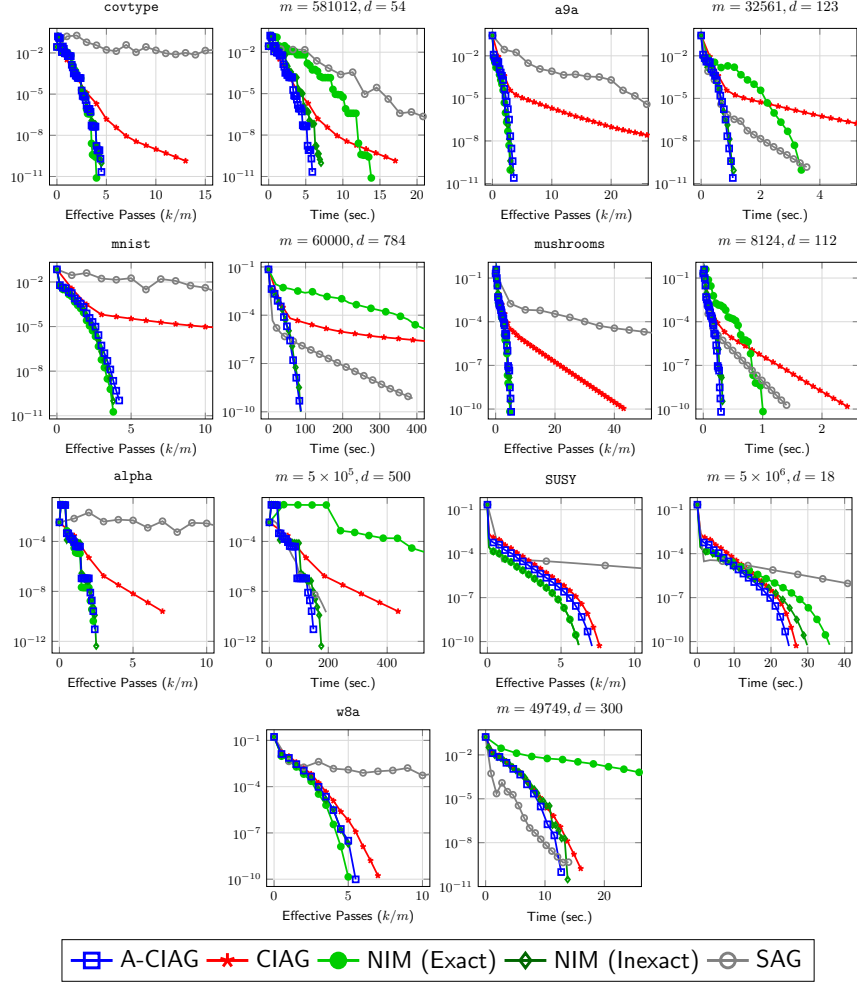


FIG. 3. Evolution of  $\|\nabla F(\theta^k)\|$  (y-axis) against number of effective passes and wall clock time on the datasets. The experiment settings are the same as in Table 2.

$\|\nabla F(\theta^k)\|$  against the number of effective passes and wall clock time on the tested datasets. As seen, the convergence speed of A-CIAG matches that of the Newton-based NIM, yet the wall clock time required is faster as it does not involve computing the Hessians' inverse; and the CIAG method exhibits a slower convergence than A-CIAG in these cases. Moreover, it is worthwhile pointing out that except for the datasets **covtype** and **alpha**, the SAG method already achieves a solution accuracy of  $\|\nabla F(\theta^k)\| \leq 10^{-6}$  in less wall clock time than the proposed methods. The benefits of our proposed methods are significant only when the solution accuracy is high. This also corroborates with our analytical results in Theorem 4.4 and 4.5.

**6. Conclusions.** We have proposed two new optimization methods utilizing the technique of curvature-aided gradient tracking for large-scale optimization via incremental data processing. The proposed methods, CIAG and A-CIAG, attain an  $\epsilon$ -optimal solution with only  $\mathcal{O}(\kappa(F) \log(1/\epsilon))$  and  $\mathcal{O}(\sqrt{\kappa(F)} \log(1/\epsilon))$  iterations, respectively, for a small  $\epsilon$ , provided that the initialization is close to optimal. Numerical experiments on real and synthetic data demonstrate the benefit of our algorithms when the required solution accuracy is high. Future work includes extending the proposed methods to composite function minimization and deriving approximation scheme to the Hessian-vector products for further acceleration in computation speed, e.g., similar to [13]. The source codes used for this

paper can be found on <http://github.com/hoitowai/ciag/>.

**Appendix A. Proof of Proposition 4.6.** The following analysis largely follows from [16, Section 3.3] and is repeated here for self-containedness. To begin, expanding  $V^{(k+1)} = \|\boldsymbol{\theta}^{k+1} - \boldsymbol{\theta}^*\|^2$  using  $\boldsymbol{\theta}^{k+1} = \boldsymbol{\theta}^k - \gamma(\nabla F(\boldsymbol{\theta}^k) + \mathbf{e}_{\text{CIAG}}^k)$  yields:

$$\begin{aligned}
 V^{(k+1)} &= V^{(k)} - 2\gamma\langle \nabla F(\boldsymbol{\theta}^k), \boldsymbol{\theta}^k - \boldsymbol{\theta}^* \rangle + \gamma^2 \|\nabla F(\boldsymbol{\theta}^k)\|^2 \\
 &\quad + \gamma^2 \|\mathbf{e}_{\text{CIAG}}^k\|^2 + 2\gamma\sqrt{V^{(k)}} \|\mathbf{e}_{\text{CIAG}}^k\| \\
 &\stackrel{(a)}{\leq} V^{(k)} - 2\gamma\left(\frac{\mu L}{\mu + L}V^{(k)} + \frac{1}{\mu + L}\|\nabla F(\boldsymbol{\theta}^k)\|^2\right) + \gamma^2 \|\nabla F(\boldsymbol{\theta}^k)\|^2 \\
 &\quad + \gamma^2 \|\mathbf{e}_{\text{CIAG}}^k\|^2 + 2\gamma\sqrt{V^{(k)}} \|\mathbf{e}_{\text{CIAG}}^k\| \\
 &= \left(1 - 2\gamma\frac{\mu L}{\mu + L}\right)V^{(k)} + \left(\gamma^2 - \frac{2\gamma}{\mu + L}\right)\|\nabla F(\boldsymbol{\theta}^k)\|^2 \\
 &\quad + \gamma^2 \|\mathbf{e}_{\text{CIAG}}^k\|^2 + 2\gamma\sqrt{V^{(k)}} \|\mathbf{e}_{\text{CIAG}}^k\| \\
 &\stackrel{(b)}{\leq} \left(1 - 2\gamma\frac{\mu L}{\mu + L}\right)V^{(k)} + \gamma^2 \|\mathbf{e}_{\text{CIAG}}^k\|^2 + 2\gamma\sqrt{V^{(k)}} \|\mathbf{e}_{\text{CIAG}}^k\|,
 \end{aligned}
 \tag{A.1}$$

where (a) is due to the strong convexity of  $F(\boldsymbol{\theta})$  [cf. Assumption 4.2] and (b) is due to the choice of step size  $\gamma \leq 2/(\mu + L)$ .

**Appendix B. Proof of Proposition 4.8.** Let us express the gradient error as  $\mathbf{e}_{\text{CIAG}}^k = \sum_{i=1}^m (\nabla f_i(\boldsymbol{\theta}^{\tau_i^k}) + \nabla^2 f_i(\boldsymbol{\theta}^{\tau_i^k})(\boldsymbol{\theta}^k - \boldsymbol{\theta}^{\tau_i^k}) - \nabla f_i(\boldsymbol{\theta}^k))$ . Applying Lemma 2.1:

$$\begin{aligned}
 \|\mathbf{e}_{\text{CIAG}}^k\| &\leq \sum_{i=1}^m \frac{L_{H,i}}{2} \|\boldsymbol{\theta}^{\tau_i^k} - \boldsymbol{\theta}^k\|^2 \leq \sum_{i=1}^m \frac{L_{H,i}}{2} \underbrace{(k - \tau_i^k)}_{\leq K} \sum_{j=\tau_i^k}^{k-1} \|\boldsymbol{\theta}^{j+1} - \boldsymbol{\theta}^j\|^2 \\
 &\leq \frac{KL_H}{2} \sum_{j=(k-K)_{++}}^{k-1} \|\boldsymbol{\theta}^{j+1} - \boldsymbol{\theta}^j\|^2 \leq \frac{KL_H}{2} \gamma^2 \sum_{j=(k-K)_{++}}^{k-1} \|\mathbf{e}_{\text{CIAG}}^j + \nabla F(\boldsymbol{\theta}^j)\|^2 \\
 &\leq \gamma^2 KL_H \sum_{j=(k-K)_{++}}^{k-1} (\|\mathbf{e}_{\text{CIAG}}^j\|^2 + \|\nabla F(\boldsymbol{\theta}^j)\|^2).
 \end{aligned}
 \tag{B.1}$$

Furthermore, we have

$$\|\nabla F(\boldsymbol{\theta}^j)\|^2 = \|\nabla F(\boldsymbol{\theta}^j) - \nabla F(\boldsymbol{\theta}^*)\|^2 \leq L^2 V^{(j)}, \quad \text{and}
 \tag{B.2}$$

$$\|\mathbf{e}_{\text{CIAG}}^j\| \leq \sum_{i=1}^m \frac{L_{H,i}}{2} \|\boldsymbol{\theta}^j - \boldsymbol{\theta}^{\tau_i^j}\|^2 \stackrel{(a)}{\leq} \sum_{i=1}^m L_{H,i} (V^{(j)} + V^{(\tau_i^j)}) \leq 2L_H \max_{\ell \in \{\tau_i^j\}_{i=1}^m \cup \{j\}} V^{(\ell)},
 \tag{B.3}$$

where (a) is due to the inequality  $\|\mathbf{a} - \mathbf{b}\|^2 \leq 2(\|\mathbf{a}\|^2 + \|\mathbf{b}\|^2)$ . Plugging these back into (B.1) gives:

$$\begin{aligned}
 \|\mathbf{e}_{\text{CIAG}}^k\| &\leq \gamma^2 KL_H \sum_{j=(k-K)_{++}}^{k-1} \left( L^2 V^{(j)} + \left( 2L_H \max_{\ell \in \{\tau_i^j\}_{i=1}^m \cup \{j\}} V^{(\ell)} \right)^2 \right) \\
 &\leq \gamma^2 K^2 L_H \left( L^2 \max_{(k-K)_{++} \leq \ell \leq k-1} V^{(\ell)} + 4L_H^2 \max_{(k-2K)_{++} \leq \ell \leq k-1} (V^{(\ell)})^2 \right),
 \end{aligned}
 \tag{B.4}$$

where in the last inequality we have used  $\tau_i^{k-K} \geq k - 2K$ .

**Appendix C. Step 3 in the Proof of Theorem 4.4.** Combining Proposition 4.6 and 4.8 yields

$$\begin{aligned}
 V^{(k+1)} &\leq \left(1 - 2\gamma \frac{\mu L}{\mu + L}\right) V^{(k)} + \gamma^2 \|e_{\text{CIAG}}^k\|^2 + 2\gamma \sqrt{V^{(k)}} \|e_{\text{CIAG}}^k\| \\
 &\leq \left(1 - 2\gamma \frac{\mu L}{\mu + L}\right) V^{(k)} \\
 &\quad + 2\gamma^3 K^2 L_H \left( L^2 \max_{(k-K)_{++} \leq \ell \leq k} (V^{(\ell)})^{\frac{3}{2}} + 4L_H^2 \max_{(k-2K)_{++} \leq \ell \leq k} (V^{(\ell)})^{\frac{5}{2}} \right) \\
 &\quad + 2\gamma^6 K^4 L_H^2 \left( L^4 \max_{(k-K)_{++} \leq \ell \leq k-1} (V^{(\ell)})^2 + 16L_H^4 \max_{(k-2K)_{++} \leq \ell \leq k-1} (V^{(\ell)})^4 \right),
 \end{aligned}
 \tag{C.1}$$

which is the exact form for Eq. (4.17). The right hand side in (C.1) can be decomposed into two terms — the first term is of the same order as  $V^{(k)}$ , and the other terms are *delayed* and *higher-order* terms of  $V^{(\ell)}$ .

Observe that (C.1) is a special case of (4.21) in Proposition 4.10 with  $R^{(k)} = V^{(k)}$ ,  $M = 2K + 1$ ,  $p = 1 - 2\gamma\mu L/(\mu + L)$  and

$$\begin{aligned}
 q_1 &= 2\gamma^3 K^2 L^2 L_H, \quad \eta_1 = 3/2, \quad q_2 = 8\gamma^3 K^2 L_H^3, \quad \eta_3 = 5/2, \\
 q_3 &= 2\gamma^6 K^4 L_H^2 L^4, \quad \eta_3 = 2, \quad q_4 = 32\gamma^6 K^4 L_H^6, \quad \eta_4 = 4.
 \end{aligned}
 \tag{C.2}$$

The corresponding convergence condition in (4.22) can be satisfied if

$$\begin{aligned}
 \gamma^5 2K^4 L_H^2 \left( L^4 V^{(1)} + 16L_H^4 (V^{(1)})^3 \right) &< \frac{\mu L}{\mu + L} \\
 \text{and } \gamma^2 2K^2 L_H \left( L^2 (V^{(1)})^{1/2} + 4L_H^2 (V^{(1)})^{3/2} \right) &< \frac{\mu L}{\mu + L},
 \end{aligned}
 \tag{C.3}$$

which can be implied by (4.1). The proof is thus concluded.

**Appendix D. Proof of Proposition 4.10.** The proof of the proposition is divided into two parts. We first show that under (4.22), the sequence  $\{R^{(k)}\}_{k \geq 1}$  converges linearly as in part (a) of the proposition; then we show that the rate of convergence is asymptotically given by  $p$  as in part (b) of the proposition [cf. (4.23)].

The first part of the proof is achieved using induction on all  $\ell \geq 1$  with the following statement:

$$R^{(k)} \leq \delta^\ell R^{(1)}, \quad \forall k = (\ell - 1)M + 2, \dots, \ell M + 1.
 \tag{D.1}$$

The base case when  $\ell = 1$  can be straightforwardly established:

$$\begin{aligned}
 R^{(2)} &\leq pR^{(1)} + \sum_{j=1}^J q_j (R^{(1)})^{\eta_j} \leq \delta R^{(1)}, \\
 &\vdots \\
 R^{(M+1)} &\leq pR^{(M)} + \sum_{j=1}^J q_j (R^{(0)})^{\eta_j} \leq \delta R^{(1)}.
 \end{aligned}
 \tag{D.2}$$

Suppose that the statement (D.1) is true up to  $\ell = c$ , for  $\ell = c + 1$ , we have:

$$\begin{aligned}
 R^{(cM+2)} &\leq pR^{(cM+1)} + \sum_{j=1}^J q_j \max_{k' \in [(c-1)M+2, cM+1]} (R^{(k')})^{\eta_j} \\
 &\leq p(\delta^c R^{(1)}) + \sum_{j=1}^J q_j (\delta^c R^{(1)})^{\eta_j} \leq \delta^c \left( pR^{(1)} + \sum_{j=1}^J q_j (R^{(1)})^{\eta_j} \right) \leq \delta^{c+1} R^{(1)}.
 \end{aligned}$$

Similar statement also holds for  $R^{(k)}$  with  $k = cM + 3, \dots, (c+1)M + 1$ . We thus conclude with:

$$(D.3) \quad R^{(k)} \leq \delta^{\lceil (k-1)/M \rceil} R^{(1)}, \quad \forall k \geq 1,$$

which proves the first part of the proposition.

The second part of the proof establishes the asymptotic linear rate of convergence in (4.23). We consider the upper bound sequence  $\{\bar{R}^{(k)}\}_{k \geq 1}$  such that  $\bar{R}^{(1)} = R^{(1)}$  and the inequality (4.21) is tight for  $\{\bar{R}^{(k)}\}_{k \geq 1}$ . Obviously, it also holds that  $\bar{R}^{(k)} \leq \delta^{\lceil (k-1)/M \rceil} \bar{R}^{(1)}$  for all  $k \geq 1$ . Now, observe that

$$(D.4) \quad \frac{\bar{R}^{(k+1)}}{\bar{R}^{(k)}} = p + \frac{\sum_{j=1}^J q_j \max_{k' \in [(k-M+1)_{++}, k]} (R^{(k')})^{\eta_j}}{\bar{R}^{(k)}}.$$

For any  $k' \in [k - M + 1, k]$  and any  $\eta > 1$ , we have:

$$(D.5) \quad \frac{(\bar{R}^{(k')})^\eta}{\bar{R}^{(k)}} = \frac{\bar{R}^{(k')}}{\bar{R}^{(k)}} (\bar{R}^{(k')})^{\eta-1} \leq \frac{\bar{R}^{(k')}}{\bar{R}^{(k)}} (R^{(1)})^{\eta-1} \delta^{(\lceil \frac{k'-1}{M} \rceil)(\eta-1)}.$$

Note that as  $\bar{R}^{(k+1)}/\bar{R}^{(k)} \geq p$ , we have:

$$(D.6) \quad \frac{(\bar{R}^{(k')})^\eta}{\bar{R}^{(k)}} \leq p^{-M} (R^{(1)})^{\eta-1} \delta^{(\lceil \frac{k'-1}{M} \rceil)(\eta-1)}.$$

Taking  $k \rightarrow \infty$  shows that the right hand side vanishes. As a result, we have  $\lim_{k \rightarrow \infty} \bar{R}^{(k+1)}/\bar{R}^{(k)} = p$ . This proves part (b) of the proposition.

**Appendix E. Proof of Proposition 4.7.** The following proof is partially inspired by [9, 24]. For simplicity, we shall drop the subscript ACIAG in the gradient and gradient error,  $\mathbf{g}_{\text{ACIAG}}^k$  and  $\mathbf{e}_{\text{ACIAG}}^k$ , respectively. Define the estimation sequence as:

$$(E.1) \quad \begin{aligned} \Phi_1(\boldsymbol{\theta}) &:= F(\boldsymbol{\theta}_{ex}^1) + \frac{\mu}{2} \|\boldsymbol{\theta} - \boldsymbol{\theta}_{ex}^1\|^2 \\ \Phi_{k+1}(\boldsymbol{\theta}) &:= (1 - \sqrt{\mu\gamma}) \Phi_k(\boldsymbol{\theta}) + \sqrt{\mu\gamma} \left( F(\boldsymbol{\theta}_{ex}^k) + \langle \mathbf{g}^k, \boldsymbol{\theta} - \boldsymbol{\theta}_{ex}^k \rangle + \frac{\mu}{2} \|\boldsymbol{\theta} - \boldsymbol{\theta}_{ex}^k\|^2 \right), \end{aligned}$$

where  $\mathbf{g}^k := \mathbf{b}^k + \mathbf{H}^k \boldsymbol{\theta}_{ex}^k$  is the gradient surrogate used in (3.11). Recall that  $\mathbf{e}^k := \mathbf{g}^k - \nabla F(\boldsymbol{\theta}_{ex}^k)$  is the gradient error. The following inequality, which holds for all  $\boldsymbol{\theta} \in \mathbb{R}^d$ , can be immediately obtained using (E.1) and the  $\mu$ -strong convexity of  $F(\boldsymbol{\theta})$ :

$$(E.2) \quad \begin{aligned} \Phi_{k+1}(\boldsymbol{\theta}) - F(\boldsymbol{\theta}) &= (1 - \sqrt{\mu\gamma}) \Phi_k(\boldsymbol{\theta}) - F(\boldsymbol{\theta}) \\ &\quad + \sqrt{\mu\gamma} \left( F(\boldsymbol{\theta}_{ex}^k) + \langle \nabla F(\boldsymbol{\theta}_{ex}^k) + \mathbf{e}^k, \boldsymbol{\theta} - \boldsymbol{\theta}_{ex}^k \rangle + \frac{\mu}{2} \|\boldsymbol{\theta} - \boldsymbol{\theta}_{ex}^k\|^2 \right) \\ &\leq (1 - \sqrt{\mu\gamma}) (\Phi_k(\boldsymbol{\theta}) - F(\boldsymbol{\theta})) + \sqrt{\mu\gamma} \langle \mathbf{e}^k, \boldsymbol{\theta} - \boldsymbol{\theta}_{ex}^k \rangle \\ &\leq (1 - \sqrt{\mu\gamma})^k (\Phi_1(\boldsymbol{\theta}) - F(\boldsymbol{\theta})) + \sum_{\ell=1}^k (1 - \sqrt{\mu\gamma})^{k-\ell} \sqrt{\mu\gamma} \langle \mathbf{e}^\ell, \boldsymbol{\theta} - \boldsymbol{\theta}_{ex}^\ell \rangle. \end{aligned}$$

To facilitate our development, let us denote:

$$(E.3) \quad \Phi_k^* := \min_{\boldsymbol{\theta}} \Phi_k(\boldsymbol{\theta}), \quad \mathbf{v}^k := \arg \min_{\boldsymbol{\theta}} \Phi_k(\boldsymbol{\theta}).$$

By setting  $\boldsymbol{\theta} = \boldsymbol{\theta}^*$  in (E.2), we have:

$$(E.4) \quad \begin{aligned} \Phi_{k+1}^* - F(\boldsymbol{\theta}^*) &\leq \Phi_{k+1}(\boldsymbol{\theta}^*) - F(\boldsymbol{\theta}^*) \\ &\leq (1 - \sqrt{\mu\gamma})^k \left( \frac{\mu}{2} \|\boldsymbol{\theta}^* - \boldsymbol{\theta}_{ex}^1\|^2 + F(\boldsymbol{\theta}_{ex}^1) - F(\boldsymbol{\theta}^*) \right) + \sum_{\ell=1}^k (1 - \sqrt{\mu\gamma})^{k-\ell} \sqrt{\mu\gamma} \langle \mathbf{e}^\ell, \boldsymbol{\theta}^* - \boldsymbol{\theta}_{ex}^\ell \rangle \\ &\leq 2(1 - \sqrt{\mu\gamma})^k \left( F(\boldsymbol{\theta}^1) - F(\boldsymbol{\theta}^*) \right) + \sum_{\ell=1}^k (1 - \sqrt{\mu\gamma})^{k-\ell} \sqrt{\mu\gamma} \langle \mathbf{e}^\ell, \boldsymbol{\theta}^* - \boldsymbol{\theta}_{ex}^\ell \rangle. \end{aligned}$$

Now, if  $F(\boldsymbol{\theta}^{k+1}) \leq \Phi_{k+1}^*$ , then the inequality above shows the evolution of the optimality gap  $h^{(k)}$ . This motivates our next step, relating  $F(\boldsymbol{\theta}^{k+1})$  to  $\Phi_{k+1}^*$ .

**Lower bounding  $\Phi_{k+1}^*$  in the presence of errors.** Since  $\nabla^2 \Phi_k(\boldsymbol{\theta}) = \mu \mathbf{I}$ , the function  $\Phi_k(\boldsymbol{\theta})$  is quadratic and we can represent  $\Phi_k(\boldsymbol{\theta})$  alternatively as

$$(E.5) \quad \Phi_k(\boldsymbol{\theta}) = \Phi_k^* + \frac{\mu}{2} \|\boldsymbol{\theta} - \mathbf{v}^k\|^2.$$

By substituting (E.5) into the definition of  $\Phi_{k+1}(\boldsymbol{\theta})$  in (E.1) and evaluating the first order optimality condition of the latter, we have:

$$(E.6) \quad \begin{aligned} & \sqrt{\mu\gamma}(\mathbf{g}^k + \mu(\mathbf{v}^{k+1} - \boldsymbol{\theta}_{ex}^k)) + (1 - \sqrt{\mu\gamma})\mu(\mathbf{v}^{k+1} - \mathbf{v}^k) = \mathbf{0}, \\ \implies & \mathbf{v}^{k+1} = (1 - \sqrt{\mu\gamma})\mathbf{v}^k + \sqrt{\mu\gamma}\boldsymbol{\theta}_{ex}^k - \sqrt{\frac{\gamma}{\mu}}\mathbf{g}^k. \end{aligned}$$

By setting  $\boldsymbol{\theta} = \boldsymbol{\theta}_{ex}^k$  in (E.1) and using the recursive definition of  $\Phi_{k+1}(\boldsymbol{\theta})$ , we obtain

$$(E.7) \quad \begin{aligned} \Phi_{k+1}(\boldsymbol{\theta}_{ex}^k) &= (1 - \sqrt{\mu\gamma})\Phi_k(\boldsymbol{\theta}_{ex}^k) + \sqrt{\mu\gamma}F(\boldsymbol{\theta}_{ex}^k) \\ &= (1 - \sqrt{\mu\gamma})\left(\Phi_k^* + \frac{\mu}{2}\|\boldsymbol{\theta}_{ex}^k - \mathbf{v}^k\|^2\right) + \sqrt{\mu\gamma}F(\boldsymbol{\theta}_{ex}^k), \end{aligned}$$

while setting  $\boldsymbol{\theta} = \boldsymbol{\theta}_{ex}^k$  in (E.5) and using (E.6) gives us:

$$(E.8) \quad \Phi_{k+1}(\boldsymbol{\theta}_{ex}^k) = \Phi_{k+1}^* + \frac{\mu}{2} \left( (1 - \sqrt{\mu\gamma})^2 \|\boldsymbol{\theta}_{ex}^k - \mathbf{v}^k\|^2 + \frac{\gamma}{\mu} \|\mathbf{g}^k\|^2 + 2(1 - \sqrt{\mu\gamma}) \sqrt{\frac{\gamma}{\mu}} \langle \mathbf{g}^k, \boldsymbol{\theta}_{ex}^k - \mathbf{v}^k \rangle \right).$$

Comparing the right hand side of (E.7) and (E.8) shows:

$$\begin{aligned} \Phi_{k+1}^* &= (1 - \sqrt{\mu\gamma})\left(\Phi_k^* + \frac{\mu}{2}\|\boldsymbol{\theta}_{ex}^k - \mathbf{v}^k\|^2\right) + \sqrt{\mu\gamma}F(\boldsymbol{\theta}_{ex}^k) \\ &\quad - \frac{\mu}{2} \left( (1 - \sqrt{\mu\gamma})^2 \|\boldsymbol{\theta}_{ex}^k - \mathbf{v}^k\|^2 + \frac{\gamma}{\mu} \|\mathbf{g}^k\|^2 + 2(1 - \sqrt{\mu\gamma}) \sqrt{\frac{\gamma}{\mu}} \langle \mathbf{g}^k, \boldsymbol{\theta}_{ex}^k - \mathbf{v}^k \rangle \right) \\ &= (1 - \sqrt{\mu\gamma})\Phi_k^* + \sqrt{\mu\gamma}F(\boldsymbol{\theta}_{ex}^k) + \frac{\mu}{2}(1 - \sqrt{\mu\gamma})\sqrt{\mu\gamma}\|\boldsymbol{\theta}_{ex}^k - \mathbf{v}^k\|^2 \\ &\quad - \frac{\gamma}{2}\|\mathbf{g}^k\|^2 - (1 - \sqrt{\mu\gamma})\sqrt{\mu\gamma}\langle \mathbf{g}^k, \boldsymbol{\theta}_{ex}^k - \mathbf{v}^k \rangle. \end{aligned}$$

Using the fact  $\mathbf{v}^k - \boldsymbol{\theta}_{ex}^k = (\sqrt{\mu\gamma})^{-1}(\boldsymbol{\theta}_{ex}^k - \boldsymbol{\theta}^k)$  (proven in Section E.1),

$$(E.9) \quad \begin{aligned} \Phi_{k+1}^* &= (1 - \sqrt{\mu\gamma})\Phi_k^* + \sqrt{\mu\gamma}F(\boldsymbol{\theta}_{ex}^k) + \frac{\mu}{2} \frac{1 - \sqrt{\mu\gamma}}{\sqrt{\mu\gamma}} \|\boldsymbol{\theta}_{ex}^k - \boldsymbol{\theta}^k\|^2 \\ &\quad - \frac{\gamma}{2}\|\mathbf{g}^k\|^2 - (1 - \sqrt{\mu\gamma})\langle \mathbf{g}^k, \boldsymbol{\theta}^k - \boldsymbol{\theta}_{ex}^k \rangle. \end{aligned}$$

We obtain the following chain:

$$\begin{aligned}
(E.10) \quad & F(\boldsymbol{\theta}^{k+1}) - \Phi_{k+1}^* \stackrel{(a)}{\leq} F(\boldsymbol{\theta}_{ex}^k) - \gamma \langle \nabla F(\boldsymbol{\theta}_{ex}^k), \mathbf{g}^k \rangle + \frac{L\gamma^2}{2} \|\mathbf{g}^k\|^2 - \Phi_{k+1}^* \\
& \stackrel{(b)}{=} (1 - \sqrt{\mu\gamma}) \left( F(\boldsymbol{\theta}_{ex}^k) + \langle \mathbf{g}^k, \boldsymbol{\theta}^k - \boldsymbol{\theta}_{ex}^k \rangle - \Phi_k^* \right) \\
& \quad - \gamma \langle \nabla F(\boldsymbol{\theta}_{ex}^k), \mathbf{g}^k \rangle + \frac{\gamma}{2} (1 + L\gamma) \|\mathbf{g}^k\|^2 - \frac{\mu}{2} \frac{1 - \sqrt{\mu\gamma}}{\sqrt{\mu\gamma}} \|\boldsymbol{\theta}_{ex}^k - \boldsymbol{\theta}^k\|^2 \\
& \stackrel{(c)}{=} (1 - \sqrt{\mu\gamma}) \left( F(\boldsymbol{\theta}_{ex}^k) + \langle \nabla F(\boldsymbol{\theta}_{ex}^k), \boldsymbol{\theta}^k - \boldsymbol{\theta}_{ex}^k \rangle - \Phi_k^* \right) \\
& \quad - \gamma \langle \nabla F(\boldsymbol{\theta}_{ex}^k), \mathbf{g}^k \rangle + (1 - \sqrt{\mu\gamma}) \langle \mathbf{e}^k, \boldsymbol{\theta}^k - \boldsymbol{\theta}_{ex}^k \rangle \\
& \quad + \frac{\gamma}{2} (1 + L\gamma) \|\mathbf{g}^k\|^2 - \frac{\mu}{2} \frac{1 - \sqrt{\mu\gamma}}{\sqrt{\mu\gamma}} \|\boldsymbol{\theta}_{ex}^k - \boldsymbol{\theta}^k\|^2 \\
& \stackrel{(d)}{\leq} (1 - \sqrt{\mu\gamma}) (F(\boldsymbol{\theta}^k) - \Phi_k^* + \langle \mathbf{e}^k, \boldsymbol{\theta}^k - \boldsymbol{\theta}_{ex}^k \rangle) - \frac{\mu}{2} \frac{1 - \mu\gamma}{\sqrt{\mu\gamma}} \|\boldsymbol{\theta}_{ex}^k - \boldsymbol{\theta}^k\|^2 \\
& \quad + \frac{\gamma}{2} (1 + L\gamma) \|\mathbf{g}^k\|^2 - \gamma \langle \nabla F(\boldsymbol{\theta}_{ex}^k), \mathbf{g}^k \rangle \\
& \stackrel{(e)}{\leq} (1 - \sqrt{\mu\gamma}) (F(\boldsymbol{\theta}^k) - \Phi_k^* + \langle \mathbf{e}^k, \boldsymbol{\theta}^k - \boldsymbol{\theta}_{ex}^k \rangle) - \frac{\mu}{2} \frac{1 - \mu\gamma}{\sqrt{\mu\gamma}} \|\boldsymbol{\theta}_{ex}^k - \boldsymbol{\theta}^k\|^2 + \gamma \|\mathbf{e}^k\|^2,
\end{aligned}$$

where (a) is due to the  $L$ -smoothness of  $F$ ; (b) is due to (E.9); (c) is obtained by expanding  $\mathbf{g}^k$  as  $\nabla F(\boldsymbol{\theta}_{ex}^k) + \mathbf{e}^k$ ; (d) is obtained by adding and subtracting  $(\mu/2)\|\boldsymbol{\theta}^k - \boldsymbol{\theta}_{ex}^k\|^2$  inside the first bracket, applying the identity  $(1 - \sqrt{\mu\gamma}) + (1 - \sqrt{\mu\gamma})/\sqrt{\mu\gamma} = (1 - \mu\gamma)/\sqrt{\mu\gamma}$ , and using the  $\mu$ -strong convexity of  $F$ ; and (e) is due to the following chain of inequalities:

$$\begin{aligned}
(E.11) \quad & \frac{\gamma}{2} (1 + L\gamma) \|\mathbf{g}^k\|^2 - \gamma \langle \nabla F(\boldsymbol{\theta}_{ex}^k), \mathbf{g}^k \rangle \\
& = \frac{\gamma}{2} (1 + L\gamma) \left( \|\mathbf{e}^k\|^2 + \|\nabla F(\boldsymbol{\theta}_{ex}^k)\|^2 + 2 \langle \nabla F(\boldsymbol{\theta}_{ex}^k), \mathbf{e}^k \rangle \right) - \gamma \|\nabla F(\boldsymbol{\theta}_{ex}^k)\|^2 - \gamma \langle \nabla F(\boldsymbol{\theta}_{ex}^k), \mathbf{e}^k \rangle \\
& = \frac{\gamma}{2} (1 + L\gamma) \left( \|\mathbf{e}^k\|^2 + \|\nabla F(\boldsymbol{\theta}_{ex}^k)\|^2 \right) + L\gamma^2 \langle \nabla F(\boldsymbol{\theta}_{ex}^k), \mathbf{e}^k \rangle - \gamma \|\nabla F(\boldsymbol{\theta}_{ex}^k)\|^2 \\
& \leq \frac{\gamma}{2} (1 + L\gamma) \left( \|\mathbf{e}^k\|^2 + \|\nabla F(\boldsymbol{\theta}_{ex}^k)\|^2 \right) + \frac{L\gamma^2}{2} \left( \|\nabla F(\boldsymbol{\theta}_{ex}^k)\|^2 + \|\mathbf{e}^k\|^2 \right) - \gamma \|\nabla F(\boldsymbol{\theta}_{ex}^k)\|^2 \\
& = \left( \frac{\gamma}{2} + L\gamma^2 \right) \|\mathbf{e}^k\|^2 + \left( -\frac{\gamma}{2} + L\gamma^2 \right) \|\nabla F(\boldsymbol{\theta}_{ex}^k)\|^2 \leq \gamma \|\mathbf{e}^k\|^2,
\end{aligned}$$

where the last inequality holds because of  $\gamma \leq 1/(2L)$ .

As  $\Phi_1(\boldsymbol{\theta}^1) = F(\boldsymbol{\theta}^1) = \Phi_1^*$ , applying the inequality (E.10) recursively shows:

$$\begin{aligned}
(E.12) \quad & F(\boldsymbol{\theta}^{k+1}) - \Phi_{k+1}^* \leq \\
& \sum_{\ell=1}^k (1 - \sqrt{\mu\gamma})^{k-\ell} \left( (1 - \sqrt{\mu\gamma}) \langle \mathbf{e}^\ell, \boldsymbol{\theta}^\ell - \boldsymbol{\theta}_{ex}^\ell \rangle + \gamma \|\mathbf{e}^\ell\|^2 - \frac{\mu}{2} \frac{1 - \mu\gamma}{\sqrt{\mu\gamma}} \|\boldsymbol{\theta}_{ex}^\ell - \boldsymbol{\theta}^\ell\|^2 \right).
\end{aligned}$$

Importantly, (E.12) establishes a lower bound on  $\Phi_{k+1}^*$  in terms of  $F(\boldsymbol{\theta}^{k+1})$  and  $\mathbf{e}^k$ .

**Proving Proposition 4.7.** Summing up (E.12) and (E.4) gives:

$$\begin{aligned}
h^{(k+1)} &\leq 2(1 - \sqrt{\mu\gamma})^k h^{(1)} + \sum_{\ell=1}^k (1 - \sqrt{\mu\gamma})^{k-\ell} \left( \sqrt{\mu\gamma} \langle \mathbf{e}^\ell, \boldsymbol{\theta}^\star - \boldsymbol{\theta}_{ex}^\ell \rangle \right. \\
&\quad \left. + (1 - \sqrt{\mu\gamma}) \langle \mathbf{e}^\ell, \boldsymbol{\theta}^\ell - \boldsymbol{\theta}_{ex}^\ell \rangle + \gamma \|\mathbf{e}^\ell\|^2 - \frac{\mu}{2} \frac{1 - \mu\gamma}{\sqrt{\mu\gamma}} \|\boldsymbol{\theta}_{ex}^\ell - \boldsymbol{\theta}^\ell\|^2 \right) \\
&= 2(1 - \sqrt{\mu\gamma})^k h^{(1)} + \sum_{\ell=1}^k (1 - \sqrt{\mu\gamma})^{k-\ell} \left( \sqrt{\mu\gamma} \langle \mathbf{e}^\ell, \boldsymbol{\theta}^\star - \boldsymbol{\theta}^\ell \rangle \right. \\
&\quad \left. + \langle \mathbf{e}^\ell, \boldsymbol{\theta}^\ell - \boldsymbol{\theta}_{ex}^\ell \rangle + \gamma \|\mathbf{e}^\ell\|^2 - \frac{\mu}{2} \frac{1 - \mu\gamma}{\sqrt{\mu\gamma}} \|\boldsymbol{\theta}_{ex}^\ell - \boldsymbol{\theta}^\ell\|^2 \right).
\end{aligned}$$

Let us take a look at the last summands in the above inequality: for any  $\ell \geq 1$ ,

$$\begin{aligned}
&\sqrt{\mu\gamma} \langle \mathbf{e}^\ell, \boldsymbol{\theta}^\star - \boldsymbol{\theta}^\ell \rangle + \langle \mathbf{e}^\ell, \boldsymbol{\theta}^\ell - \boldsymbol{\theta}_{ex}^\ell \rangle + \gamma \|\mathbf{e}^\ell\|^2 - \frac{\mu}{2} \frac{1 - \mu\gamma}{\sqrt{\mu\gamma}} \|\boldsymbol{\theta}_{ex}^\ell - \boldsymbol{\theta}^\ell\|^2 \\
&\stackrel{(a)}{\leq} \sqrt{\mu\gamma} \|\mathbf{e}^\ell\| \|\boldsymbol{\theta}^\star - \boldsymbol{\theta}^\ell\| + \left( \gamma + \frac{\sqrt{\gamma/\mu}}{1 - \mu\gamma} \right) \|\mathbf{e}^\ell\|^2 - \frac{\mu}{4} \frac{1 - \mu\gamma}{\sqrt{\mu\gamma}} \|\boldsymbol{\theta}_{ex}^\ell - \boldsymbol{\theta}^\ell\|^2 \\
&\stackrel{(b)}{\leq} \sqrt{2\gamma h^{(\ell)}} \|\mathbf{e}^\ell\| + \left( \gamma + \frac{\sqrt{\gamma/\mu}}{1 - \mu\gamma} \right) \|\mathbf{e}^\ell\|^2 - \frac{\mu}{4} \frac{1 - \mu\gamma}{\sqrt{\mu\gamma}} \|\boldsymbol{\theta}_{ex}^\ell - \boldsymbol{\theta}^\ell\|^2 \\
&\stackrel{(c)}{\leq} \sqrt{2\gamma h^{(\ell)}} \|\mathbf{e}^\ell\| + \sqrt{\frac{9\gamma}{\mu}} \|\mathbf{e}^\ell\|^2 - \frac{\mu}{4} \frac{1 - \mu\gamma}{\sqrt{\mu\gamma}} \|\boldsymbol{\theta}_{ex}^\ell - \boldsymbol{\theta}^\ell\|^2,
\end{aligned} \tag{E.13}$$

where (a) is resulted from the fact  $\langle \mathbf{e}^\ell, \boldsymbol{\theta}^\ell - \boldsymbol{\theta}_{ex}^\ell \rangle \leq (1/2)(\|\mathbf{e}^\ell\|^2/c + c\|\boldsymbol{\theta}^\ell - \boldsymbol{\theta}_{ex}^\ell\|^2)$  for any  $c > 0$  and we have set  $c = \frac{\mu}{2} \frac{1 - \mu\gamma}{\sqrt{\mu\gamma}}$  therein; (b) is due to the relation  $\|\boldsymbol{\theta}^\ell - \boldsymbol{\theta}^\star\| \leq \sqrt{2h^{(\ell)}/\mu}$ ; (c) is due to  $\gamma + \frac{\sqrt{\gamma/\mu}}{1 - \mu\gamma} \leq 3\sqrt{\gamma/\mu}$ , which can be verified through replacing  $\gamma$  by its upper bound  $1/(2L)$  in the denominator of the fraction on the left-hand-side. Combining the two equations above yields the result.

**E.1. Proof of Equality.** We prove  $\mathbf{v}^k - \boldsymbol{\theta}_{ex}^k = (\sqrt{\mu\gamma})^{-1}(\boldsymbol{\theta}_{ex}^k - \boldsymbol{\theta}^k)$  using induction on  $k$ . Clearly, the said equality holds for  $k = 1$  since  $\mathbf{v}^1 = \boldsymbol{\theta}^1 = \boldsymbol{\theta}_{ex}^1$ , and we assume that it holds up to  $k$ . Consider:

$$\begin{aligned}
\mathbf{v}^{k+1} - \boldsymbol{\theta}_{ex}^{k+1} &= (1 - \sqrt{\mu\gamma})\mathbf{v}^k + \sqrt{\mu\gamma}\boldsymbol{\theta}_{ex}^k - \sqrt{\frac{\gamma}{\mu}}\mathbf{g}^k - \boldsymbol{\theta}_{ex}^{k+1} \\
&= (1 - \sqrt{\mu\gamma})(\mathbf{v}^k - \boldsymbol{\theta}_{ex}^k) + \boldsymbol{\theta}_{ex}^k - \sqrt{\frac{\gamma}{\mu}}\mathbf{g}^k - \boldsymbol{\theta}_{ex}^{k+1} \\
&= \frac{1 - \sqrt{\mu\gamma}}{\sqrt{\mu\gamma}}(\boldsymbol{\theta}_{ex}^k - \boldsymbol{\theta}^k) + \boldsymbol{\theta}_{ex}^k - \sqrt{\frac{\gamma}{\mu}}\mathbf{g}^k - \boldsymbol{\theta}_{ex}^{k+1},
\end{aligned} \tag{E.14}$$

where we have used the induction hypothesis. Furthermore, using  $\boldsymbol{\theta}^{k+1} = \boldsymbol{\theta}_{ex}^k - \gamma\mathbf{g}^k$ ,

$$\begin{aligned}
\mathbf{v}^{k+1} - \boldsymbol{\theta}_{ex}^{k+1} &= \sqrt{\mu\gamma}^{-1} \left( (1 - \sqrt{\mu\gamma})(\boldsymbol{\theta}_{ex}^k - \boldsymbol{\theta}^k) + \sqrt{\mu\gamma}(\boldsymbol{\theta}_{ex}^k - \boldsymbol{\theta}_{ex}^{k+1}) - \gamma\mathbf{g}^k \right) \\
&= \sqrt{\mu\gamma}^{-1} \left( \boldsymbol{\theta}^{k+1} - (1 - \sqrt{\mu\gamma})\boldsymbol{\theta}^k - \sqrt{\mu\gamma}\boldsymbol{\theta}_{ex}^{k+1} \right) \\
&= \sqrt{\mu\gamma}^{-1} \left( \sqrt{\mu\gamma}(\boldsymbol{\theta}^{k+1} - \boldsymbol{\theta}_{ex}^{k+1}) + (1 - \sqrt{\mu\gamma})(\boldsymbol{\theta}^{k+1} - \boldsymbol{\theta}^k) \right) \\
&= \sqrt{\mu\gamma}^{-1} (\boldsymbol{\theta}_{ex}^{k+1} - \boldsymbol{\theta}^{k+1}),
\end{aligned} \tag{E.15}$$

where the second last equality is due to the identity  $(1 - \sqrt{\mu\gamma})(\boldsymbol{\theta}^{k+1} - \boldsymbol{\theta}^k) = (1 + \sqrt{\mu\gamma})(\boldsymbol{\theta}_{ex}^{k+1} - \boldsymbol{\theta}^{k+1})$ . The equality is thus proven.

**Appendix F. Proof of Proposition 4.9.** We begin by observing that due to the  $L_{H,i}$ -Lipschitz continuity of the Hessian of  $f_i$  and using Lemma 2.1, we have:

$$(F.1) \quad \|\mathbf{e}_{\text{ACIAG}}^\ell\| = \|\mathbf{g}_{\text{ACIAG}}^\ell - \nabla F(\boldsymbol{\theta}_{ex}^\ell)\| \leq \sum_{i=1}^m \frac{L_{H,i}}{2} \|\boldsymbol{\theta}_{ex}^\ell - \boldsymbol{\theta}_{ex}^{\tau_i^\ell}\|^2.$$

Now, expanding the right hand side of (F.1) gives:

$$(F.2) \quad \begin{aligned} \|\mathbf{e}_{\text{ACIAG}}^\ell\| &\leq \sum_{i=1}^m \frac{L_{H,i}}{2} \|\boldsymbol{\theta}_{ex}^\ell - \boldsymbol{\theta}_{ex}^{\tau_i^\ell}\|^2 \leq \sum_{i=1}^m \frac{L_{H,i}}{2} \underbrace{(\ell - \tau_i^\ell)}_{\leq K} \sum_{j=\ell-\tau_i^\ell}^{\ell-1} \|\boldsymbol{\theta}_{ex}^{j+1} - \boldsymbol{\theta}_{ex}^j\|^2 \\ &\leq \frac{KL_H}{2} \sum_{j=(\ell-K)_{++}}^{\ell-1} \|\boldsymbol{\theta}_{ex}^{j+1} - \boldsymbol{\theta}_{ex}^j\|^2 = \frac{KL_H}{2} \sum_{j=(\ell-K)_{++}}^{\ell-1} \|\gamma \mathbf{g}_{\text{ACIAG}}^j + \underbrace{\alpha(\boldsymbol{\theta}^{j+1} - \boldsymbol{\theta}^j)}_{=\boldsymbol{\theta}_{ex}^{j+1} - \boldsymbol{\theta}_{ex}^j}\|^2 \\ &\leq \frac{3KL_H}{2} \sum_{j=(\ell-K)_{++}}^{\ell-1} \left( \gamma^2 (\|\mathbf{e}^j\|^2 + \|\nabla F(\boldsymbol{\theta}_{ex}^j)\|^2) + \|\boldsymbol{\theta}_{ex}^{j+1} - \boldsymbol{\theta}^{j+1}\|^2 \right). \end{aligned}$$

Remarkably, the above bound resembles that of Proposition 4.8 with the exception of the last term that depends on  $\boldsymbol{\theta}_{ex}^{j+1} - \boldsymbol{\theta}^{j+1}$ . This is included to account for the extrapolated iterates used in the A-CIAG method.

To find an upper bound of  $\|\mathbf{e}_{\text{ACIAG}}^\ell\|$  to corroborate Proposition 4.9, in what follows, we will upper bound  $\|\mathbf{e}_{\text{ACIAG}}^j\|^2$  and  $\|\nabla F(\boldsymbol{\theta}_{ex}^j)\|^2$ , respectively. Firstly,

$$(F.3) \quad \begin{aligned} \|\mathbf{e}_{\text{ACIAG}}^j\| &\leq \sum_{i=1}^m \frac{L_{H,i}}{2} \|\boldsymbol{\theta}_{ex}^j - \boldsymbol{\theta}_{ex}^{\tau_i^j}\|^2 = \sum_{i=1}^m \frac{L_{H,i}}{2} \|\boldsymbol{\theta}^j + \alpha(\boldsymbol{\theta}^j - \boldsymbol{\theta}^{j-1}) - \boldsymbol{\theta}^{\tau_i^j} - \alpha(\boldsymbol{\theta}^{\tau_i^j} - \boldsymbol{\theta}^{\tau_i^j-1})\|^2 \\ &\leq \sum_{i=1}^m L_{H,i} \left( (1 + \alpha)^2 \|\boldsymbol{\theta}^j - \boldsymbol{\theta}^{\tau_i^j}\|^2 + \alpha^2 \|\boldsymbol{\theta}^{j-1} - \boldsymbol{\theta}^{\tau_i^j-1}\|^2 \right). \end{aligned}$$

Noticing that as  $\|\boldsymbol{\theta}^j - \boldsymbol{\theta}^{\tau_i^j}\|^2 \leq 2(\|\boldsymbol{\theta}^j - \boldsymbol{\theta}^*\|^2 + \|\boldsymbol{\theta}^{\tau_i^j} - \boldsymbol{\theta}^*\|^2) \leq (4/\mu)(h^{(j)} + h^{(\tau_i^j)})$ , it follows from (F.3) that

$$(F.4) \quad \begin{aligned} \|\mathbf{e}_{\text{ACIAG}}^j\| &\leq \frac{4}{\mu} \sum_{i=1}^m L_{H,i} \left( (1 + \alpha)^2 (h^{(j)} + h^{(\tau_i^j)}) + \alpha^2 (h^{(j-1)} + h^{(\tau_i^j-1)}) \right) \\ &\leq \frac{8L_H}{\mu} ((1 + \alpha)^2 + \alpha^2) \max_{(j-K-1)_{++} \leq q \leq j} h^{(q)} \leq \frac{40L_H}{\mu} \max_{(j-K-1)_{++} \leq q \leq j} h^{(q)}, \end{aligned}$$

which implies

$$(F.5) \quad \begin{aligned} \sum_{j=(\ell-K)_{++}}^{\ell-1} \|\mathbf{e}_{\text{ACIAG}}^j\|^2 &\leq \sum_{j=(\ell-K)_{++}}^{\ell-1} \left( \frac{40L_H}{\mu} \right)^2 \max_{(j-K-1)_{++} \leq q \leq j} (h^{(q)})^2 \\ &\leq K \left( \frac{40L_H}{\mu} \right)^2 \max_{(\ell-2K-1)_{++} \leq q \leq \ell} (h^{(q)})^2. \end{aligned}$$

Secondly,

$$(F.6) \quad \|\nabla F(\boldsymbol{\theta}_{ex}^j)\|^2 \leq 2L^2 (\|\boldsymbol{\theta}^j - \boldsymbol{\theta}^*\|^2 + \|\boldsymbol{\theta}^j - \boldsymbol{\theta}^{j-1}\|^2) \leq \frac{4L^2}{\mu} (3h^{(j)} + 2h^{(j-1)}),$$

thus

$$(F.7) \quad \sum_{j=(\ell-K)_{++}}^{\ell-1} \|\nabla F(\boldsymbol{\theta}_{ex}^j)\|^2 \leq \sum_{j=(\ell-K)_{++}}^{\ell-1} \frac{4L^2}{\mu} \left(3h^{(j)} + 2h^{(j-1)}\right) \leq \frac{20L^2K}{\mu} \max_{(\ell-K-1)_{++} \leq q \leq \ell-1} h^{(q)}.$$

Substituting (F.5) and (F.7) into the right hand side of (F.2) verifies Proposition 4.9.

**Appendix G. Step 3 in the Proof of Theorem 4.5.** To proceed with the proof, we show in the following a bound on  $\|e_{ACIAG}^\ell\|^2$ , which can be derived directly from Proposition 4.9:

$$(G.1) \quad \begin{aligned} \|e_{ACIAG}^\ell\|^2 &\leq \frac{27K^3L_H^2}{4} \sum_{j=(\ell-K)_{++}}^{\ell-1} \|\boldsymbol{\theta}^{j+1} - \boldsymbol{\theta}_{ex}^{j+1}\|^4 \\ &\quad + \gamma^4 \frac{27K^4L_H^2}{4} \left(\frac{20L^2}{\mu}\right)^2 \max_{(\ell-K-1)_{++} \leq q \leq \ell-1} (h^{(q)})^2 \\ &\quad + \gamma^4 \frac{27K^4L_H^2}{4} \left(\frac{40L_H}{\mu}\right)^4 \max_{(\ell-2K-1)_{++} \leq q \leq \ell-1} (h^{(q)})^4. \end{aligned}$$

The bracket inside the right hand side of (4.14) in Proposition 4.7 can be bounded using Proposition 4.9 and (G.1) as:

$$(G.2) \quad \begin{aligned} &\sqrt{2\gamma h^{(\ell)}} \|e_{ACIAG}^\ell\| + \sqrt{\frac{9\gamma}{\mu}} \|e_{ACIAG}^\ell\|^2 - \frac{\mu}{4} \frac{1-\mu\gamma}{\sqrt{\mu\gamma}} \|\boldsymbol{\theta}_{ex}^\ell - \boldsymbol{\theta}^\ell\|^2 \\ &\leq \sqrt{\frac{9\gamma h^{(\ell)} K^2 L_H^2}{2}} \left( \sum_{j=(\ell-K+1)_{++}}^{\ell} \|\boldsymbol{\theta}^j - \boldsymbol{\theta}_{ex}^j\|^2 + \gamma^2 K \left(\frac{40L_H}{\mu}\right)^2 \max_{(\ell-2K-1)_{++} \leq q \leq \ell} (h^{(q)})^2 \right. \\ &\quad \left. + \frac{20L^2}{\mu} \max_{(\ell-K-1)_{++} \leq q \leq \ell} h^{(q)} \right) \\ &\quad + \frac{27K^3L_H^2}{4} \sqrt{\frac{9\gamma}{\mu}} \left( \sum_{j=(\ell-K+1)_{++}}^{\ell} \|\boldsymbol{\theta}^j - \boldsymbol{\theta}_{ex}^j\|^4 + \gamma^4 K \left(\frac{40L_H}{\mu}\right)^4 \max_{(\ell-2K-1)_{++} \leq q \leq \ell} (h^{(q)})^4 \right. \\ &\quad \left. + \left(\frac{20L^2}{\mu}\right)^2 \max_{(\ell-K-1)_{++} \leq q \leq \ell} (h^{(q)})^2 \right) \\ &\quad - \frac{\mu}{4} \frac{1-\mu\gamma}{\sqrt{\mu\gamma}} \|\boldsymbol{\theta}^\ell - \boldsymbol{\theta}_{ex}^\ell\|^2. \end{aligned}$$

Note that the result in Proposition 4.7 is an intermediate one. We need to further bound  $h^{(k)}$  [recall for (4.14) in Proposition 4.7] in terms of itself to create a ‘recursion’ for  $h^{(k)}$ . To upper bound the right hand side of (4.14), let us start from (G.2). Define  $\rho := 1 - \sqrt{\mu\gamma}$ , it follows that

$$\begin{aligned} &\sum_{\ell=1}^k \rho^{k-\ell} \left( \sqrt{2\gamma h^{(\ell)}} \|e^\ell\| + \sqrt{\frac{9\gamma}{\mu}} \|e^\ell\|^2 - \frac{\mu}{4} \frac{1-\mu\gamma}{\sqrt{\mu\gamma}} \|\boldsymbol{\theta}_{ex}^\ell - \boldsymbol{\theta}^\ell\|^2 \right) \leq \\ &\sum_{\ell=1}^k \rho^{k-\ell} \left( \gamma^{\frac{5}{2}} \sqrt{\frac{9}{2}} K^2 L_H \left( \left(\frac{40L_H}{\mu}\right)^2 \max_{(\ell-2K-1)_{++} \leq q \leq \ell} (h^{(q)})^{\frac{5}{2}} + \frac{20L^2}{\mu} \max_{(\ell-K-1)_{++} \leq q \leq \ell} (h^{(q)})^{\frac{3}{2}} \right) \right. \\ &\quad \left. + \gamma^{\frac{9}{2}} \frac{81K^4L_H^2}{4\sqrt{\mu}} \left( \left(\frac{40L_H}{\mu}\right)^4 \max_{(\ell-2K-1)_{++} \leq q \leq \ell} (h^{(q)})^4 + \left(\frac{20L^2}{\mu}\right)^2 \max_{(\ell-K-1)_{++} \leq q \leq \ell} (h^{(q)})^2 \right) + \right. \\ &\quad \left. \left( \sum_{j=\ell}^{\min\{k, \ell+K-1\}} \left( \sqrt{\frac{9\gamma K^2 L_H^2 h^{(j)}}{2}} + \frac{81K^3L_H^2}{4} \sqrt{\frac{\gamma}{\mu}} \|\boldsymbol{\theta}^\ell - \boldsymbol{\theta}_{ex}^\ell\|^2 \right) - \frac{\mu}{4} \frac{1-\mu\gamma}{\sqrt{\mu\gamma}} \|\boldsymbol{\theta}^\ell - \boldsymbol{\theta}_{ex}^\ell\|^2 \right) \right). \end{aligned}$$

Moreover, we observe that for  $\ell \geq 2$ :

$$(G.3) \quad \|\boldsymbol{\theta}^\ell - \boldsymbol{\theta}_{ex}^\ell\|^2 \leq 2(\|\boldsymbol{\theta}^\ell - \boldsymbol{\theta}^*\|^2 + \|\boldsymbol{\theta}^{\ell-1} - \boldsymbol{\theta}^*\|^2) \leq \frac{4}{\mu}(h^{(\ell)} + h^{(\ell-1)}) ,$$

The coefficient in front of the last  $\|\boldsymbol{\theta}^\ell - \boldsymbol{\theta}_{ex}^\ell\|^2$  term can thus be upper bounded as:

$$K^2 L_H \sqrt{\frac{9\gamma}{2}} \max_{\ell \leq q \leq \min\{\ell+K-1, k\}} (h^{(q)})^{\frac{1}{2}} + \sqrt{\gamma} \frac{81K^4 L_H^2}{\mu^{\frac{3}{2}}} (h^{(\ell)} + h^{(\ell-1)}) - \frac{\mu}{4} \frac{1 - \mu\gamma}{\sqrt{\mu\gamma}} .$$

Note that (4.14) with (G.3) plugged in is an exact form of Eq. (4.20) presented in Section 4. If we define that

$$(G.4) \quad \begin{aligned} E^{(\ell, k)} := & \gamma^{\frac{5}{2}} \sqrt{\frac{9}{2}} K^2 L_H \left( \left( \frac{40L_H}{\mu} \right)^2 \max_{(\ell-2K-1)_{++} \leq q \leq \ell} (h^{(q)})^{\frac{5}{2}} + \frac{20L^2}{\mu} \max_{(\ell-K-1)_{++} \leq q \leq \ell} (h^{(q)})^{\frac{3}{2}} \right) \\ & + \gamma^{\frac{9}{2}} \frac{81K^4 L_H^2}{4\sqrt{\mu}} \left( \left( \frac{40L_H}{\mu} \right)^4 \max_{(\ell-2K-1)_{++} \leq q \leq \ell} (h^{(q)})^4 + \left( \frac{20L^2}{\mu} \right)^2 \max_{(\ell-K-1)_{++} \leq q \leq \ell} (h^{(q)})^2 \right) \\ & + \left( \gamma K^2 L_H \sqrt{\frac{9}{2}} \max_{\ell \leq q \leq \min\{\ell+K-1, k\}} (h^{(q)})^{\frac{1}{2}} + \gamma \frac{81K^4 L_H^2}{\mu^{\frac{3}{2}}} (h^{(\ell)} + h^{(\ell-1)}) \right. \\ & \quad \left. - \frac{\mu}{4} \frac{1 - \mu\gamma}{\sqrt{\mu}} \right) \frac{\|\boldsymbol{\theta}^\ell - \boldsymbol{\theta}_{ex}^\ell\|^2}{\sqrt{\gamma}} , \end{aligned}$$

where  $E^{(\ell, k)} = E^{(\ell, k-1)}$  for all  $k \geq \ell + m$ . Finally, by Proposition 4.7, we obtain

$$(G.5) \quad h^{(k+1)} \leq 2(1 - \sqrt{\mu\gamma})^k h^{(1)} + \sum_{\ell=1}^k (1 - \sqrt{\mu\gamma})^{k-\ell} E^{(\ell, k)} .$$

**Concluding the Proof of Theorem 4.5.** Our goal is to analyze (G.5) using Proposition 4.11. Let us recognize that:

$$\begin{aligned} R^{(k)} &= \bar{h}^{(k)}, \quad p = (1 - \sqrt{\mu\gamma}), \quad b = 2, \quad M = 2K + 1, \quad \eta_1 = \frac{3}{2}, \quad \eta_2 = \frac{5}{2}, \quad \eta_3 = 2, \quad \eta_4 = 4 \\ s_1 &= \gamma^{\frac{5}{2}} \sqrt{\frac{9}{2}} K^2 L_H \frac{20L^2}{\mu}, \quad s_2 = \gamma^{\frac{5}{2}} \sqrt{\frac{9}{2}} K^2 L_H \left( \frac{40L_H}{\mu} \right)^2, \\ s_3 &= \gamma^{\frac{9}{2}} \frac{81K^4 L_H^2}{4\sqrt{\mu}} \left( \frac{20L^2}{\mu} \right)^2, \quad s_4 = \gamma^{\frac{9}{2}} \frac{81K^4 L_H^2}{4\sqrt{\mu}} \left( \frac{40L_H}{\mu} \right)^4, \\ c &= \frac{\mu}{4} \frac{1 - \mu\gamma}{\sqrt{\mu}}, \quad D^{(\ell)} = \frac{\|\boldsymbol{\theta}^\ell - \boldsymbol{\theta}_{ex}^\ell\|^2}{\sqrt{\gamma}}, \quad f(\bar{h}^{(q)}) = \gamma \left( K^2 L_H \sqrt{\frac{9}{2}} (\bar{h}^{(q)})^{\frac{1}{2}} + \frac{162K^4 L_H^2}{\mu^{\frac{3}{2}}} \bar{h}^{(q)} \right) . \end{aligned}$$

The conditions in (4.28) are satisfied when

$$(G.6) \quad \begin{aligned} & \frac{\sqrt{\mu}}{4} - \gamma \left( K^2 L_H \sqrt{9} (\bar{h}^{(1)})^{\frac{1}{2}} + \frac{324K^4 L_H^2}{\mu^{\frac{3}{2}}} \bar{h}^{(1)} + \frac{\mu^{\frac{3}{2}}}{4} \right) \geq 0 \\ & \iff \gamma \leq \frac{\sqrt{\mu}}{4} \left( K^2 L_H \sqrt{9} (\bar{h}^{(1)})^{\frac{1}{2}} + \frac{324K^4 L_H^2}{\mu^{\frac{3}{2}}} \bar{h}^{(1)} + \frac{\mu^{\frac{3}{2}}}{4} \right)^{-1} := \frac{\bar{c}_3}{L} , \end{aligned}$$

and

$$(G.7) \quad \begin{aligned} 1 &> (1 - \sqrt{\mu\gamma}) + \gamma^{\frac{5}{2}} \sqrt{\frac{9}{2}} K^2 L_H \left( \frac{20L^2}{\mu} (2\bar{h}^{(1)})^{\frac{1}{2}} + \left( \frac{40L_H}{\mu} \right)^2 (2\bar{h}^{(1)})^{\frac{3}{2}} \right) \\ &+ \gamma^{\frac{9}{2}} \frac{81K^4 L_H^2}{4\sqrt{\mu}} \left( \left( \frac{20L^2}{\mu} \right)^2 (2\bar{h}^{(1)}) + \left( \frac{40L_H}{\mu} \right)^4 (2\bar{h}^{(1)})^3 \right) , \end{aligned}$$

that can be implied by

$$(G.8) \quad \begin{aligned} \gamma &< \left( \frac{\sqrt{\mu}}{\sqrt{18}K^2L_H} \left( \frac{20L^2}{\mu} (2\bar{h}^{(1)})^{\frac{1}{2}} + \left( \frac{40L_H}{\mu} \right)^2 (2\bar{h}^{(1)})^{\frac{3}{2}} \right)^{-1} \right)^{\frac{1}{2}} := \frac{\bar{c}_1}{L} \quad \text{and} \\ \gamma &< \left( \frac{2\mu}{81K^4L_H^2} \left( \left( \frac{20L^2}{\mu} \right)^2 (2\bar{h}^{(1)}) + \left( \frac{40L_H}{\mu} \right)^4 (2\bar{h}^{(1)})^3 \right)^{-1} \right)^{\frac{1}{4}} := \frac{\bar{c}_2}{L}. \end{aligned}$$

Substituting these constants into Proposition 4.11 proves the claims in Theorem 4.5.

**Appendix H. Proof of Proposition 4.11.** Define  $\{\bar{R}^{(k)}\}_{k \geq 1}$  that satisfies:

$$(H.1) \quad \bar{R}^{(k+1)} = p^k b \bar{R}^{(1)} + \sum_{\ell=1}^k p^{k-\ell} \left( \sum_{j=1}^J s_j \max_{(\ell-M)_{++} \leq q \leq \ell} (\bar{R}^{(q)})^{\eta_j} \right), \quad \bar{R}^{(1)} = R^{(1)},$$

By subtracting  $p\bar{R}^{(k)}$  from  $\bar{R}^{(k+1)}$ , (H.1) can be alternatively expressed as:

$$(H.2) \quad \bar{R}^{(k+1)} - p\bar{R}^{(k)} = \sum_{j=1}^J s_j \max_{(k-M)_{++} \leq q \leq k} (\bar{R}^{(q)})^{\eta_j}.$$

Now, consider the statements (i) and (ii) in (4.29) as the following event:

$$\mathcal{E}_z = \left\{ \bar{R}^{((z-1)M+k+1)} \geq R^{((z-1)M+k+1)}, \bar{R}^{((z-1)M+k+1)} \leq \delta^z (b\bar{R}^{(1)}), k = 1, \dots, M \right\},$$

for all  $z \geq 1$ . We shall prove that  $\mathcal{E}_z$  is true for  $z = 1, 2, \dots$  using induction.

**Base case with  $z = 1$ .** To prove  $\mathcal{E}_1$ , let us apply another induction on  $k$  inside the event. For the base case of  $k = 1$ ,

$$(H.3) \quad \bar{R}^{(2)} \geq p(bR^{(1)}) + \sum_{j=1}^J s_j (R^{(1)})^{\eta_j} - (\bar{f} - f(R^{(1)}))D^{(1)} = R^{(2)},$$

where we used the fact  $\bar{f} \geq f(bR^{(1)}) \geq f(R^{(1)})$ . Furthermore, the base case holds as:

$$(H.4) \quad \bar{R}^{(2)} = (b\bar{R}^{(1)}) \left( p + (1/b) \sum_{j=1}^J s_j (\bar{R}^{(1)})^{\eta_j-1} \right) \leq \delta(b\bar{R}^{(1)}).$$

For the induction step, suppose that the statements in (H.3) are also true up to  $k = k' - 1$  with  $z = 1$  such that  $\bar{R}^{(k')} \geq R^{(k')}$  and  $\bar{R}^{(k')} \leq \delta(b\bar{R}^{(1)})$ . Consider the case of  $k = k'$ , we observe that  $\bar{f} \geq f(bR^{(1)}) \geq f(\delta bR^{(1)}) \geq f(\bar{R}^{(q)}) \geq f(R^{(q)})$  for all  $q = 1, \dots, k'$ . Therefore, we can lower bound  $\bar{R}^{(k'+1)}$  as:

$$\begin{aligned} \bar{R}^{(k'+1)} &= p^{k'} (b\bar{R}^{(1)}) + \sum_{\ell=1}^{k'} p^{k'-\ell} \left( \sum_{j=1}^J s_j \max_{(\ell-M)_{++} \leq q \leq \ell} (\bar{R}^{(q)})^{\eta_j} \right) \\ &\geq p^{k'} (bR^{(1)}) + \sum_{\ell=1}^{k'} p^{k'-\ell} \left( \sum_{j=1}^J s_j \max_{(\ell-M)_{++} \leq q \leq \ell} (R^{(q)})^{\eta_j} - \left( \bar{f} - \max_{\ell \leq q \leq k'} f(R^{(q)}) \right) V^{(\ell)} \right) = R^{(k'+1)}, \end{aligned}$$

also, using (H.2), we can show the base case as:

$$(H.5) \quad \begin{aligned} \bar{R}^{(k'+1)} &= p\bar{R}^{(k')} + \sum_{j=1}^J s_j \max_{(k'-M)_{++} \leq q \leq k'} (\bar{R}^{(q)})^{\eta_j} \\ &\leq (b\bar{R}^{(1)}) \left( \delta p + \sum_{j=1}^J s_j (b\bar{R}^{(1)})^{\eta_j-1} \right) \leq \delta(b\bar{R}^{(1)}). \end{aligned}$$

**Induction Case.** For the induction case, suppose that  $\mathcal{E}_z$  is true for all  $z$  up to  $z'$ . We consider the case when  $z = z' + 1$ . Once again, we shall apply another induction on  $k$ . In the base case of  $k = 1$  and  $z = z' + 1$ , we have

$$\begin{aligned} \bar{R}^{(z'M+2)} &= p^{z'M+1}(b\bar{R}^{(1)}) + \sum_{\ell=1}^{z'M+1} p^{z'M+1-\ell} \left( \sum_{j=1}^J s_j \max_{(\ell-M)_{++} \leq q \leq \ell} (\bar{R}^{(q)})^{\eta_j} \right) \\ &\geq p^{z'M+1}(bR^{(1)}) + \sum_{\ell=1}^{z'M+1} p^{z'M+1-\ell} \left( \sum_{j=1}^J s_j \max_{(\ell-M)_{++} \leq q \leq \ell} (R^{(q)})^{\eta_j} \right. \\ &\quad \left. - (\bar{f} - \max_{\ell \leq q \leq z'M+1} f(R^{(q)})) V^{(\ell)} \right) = R^{(z'M+2)}, \end{aligned}$$

where we used  $\bar{f} \geq f(bR^{(1)}) \geq f(\bar{R}^{(q)}) \geq f(R^{(q)})$  for all  $q$  up to  $q = z'M + 1$  (by the induction hypothesis). Furthermore, the base case holds since:

$$\begin{aligned} \bar{R}^{(z'M+2)} &= p\bar{R}^{(z'M+1)} + \sum_{j=1}^J s_j \max_{(z'M+1-M)_{++} \leq q \leq z'M+1} (\bar{R}^{(q)})^{\eta_j} \\ (H.6) \quad &\leq \delta^{z'}(b\bar{R}^{(1)}) \left( p + \sum_{j=1}^J s_j (\delta^{z'})^{\eta_j-1} (b\bar{R}^{(1)})^{\eta_j-1} \right) \leq \delta^{z'+1}(b\bar{R}^{(1)}). \end{aligned}$$

Let the statements in  $\mathcal{E}_z$  be true up to  $k = k' - 1$ ,  $z = z' + 1$ . With  $k = k'$ ,

$$\begin{aligned} \bar{R}^{(z'M+k'+1)} &= p^{z'M+k'}(b\bar{R}^{(1)}) + \sum_{\ell=1}^{z'M+k'} p^{z'M+k'-\ell} \left( \sum_{j=1}^J s_j \max_{(\ell-M)_{++} \leq q \leq \ell} (\bar{R}^{(q)})^{\eta_j} \right) \\ &\geq p^{z'M+k'}(bR^{(1)}) + \sum_{\ell=1}^{z'M+k'} p^{z'M+k'-\ell} \left( \sum_{j=1}^J s_j \max_{(\ell-M)_{++} \leq q \leq \ell} (R^{(q)})^{\eta_j} \right. \\ &\quad \left. - (\bar{f} - \max_{\ell \leq q \leq z'M+k'} f(R^{(q)})) V^{(\ell)} \right) = R^{(z'M+k'+1)}, \\ \bar{R}^{(z'M+k'+1)} &= p\bar{R}^{(z'M+k')} + \sum_{j=1}^J s_j \max_{(z'M+k'-M)_{++} \leq q \leq z'M+k'} (\bar{R}^{(q)})^{\eta_j} \\ (H.7) \quad &\leq \delta^{z'}(b\bar{R}^{(1)}) \left( \delta p + \sum_{j=1}^J s_j (\delta^{z'})^{\eta_j-1} (b\bar{R}^{(1)})^{\eta_j-1} \right) \leq \delta^{z'+1}(b\bar{R}^{(1)}). \end{aligned}$$

The induction case is thus proven. This shows that the event  $\mathcal{E}_z$  is true for all  $z \geq 1$ .

**Proving Statement (iii).** We apply statement (ii) to prove (iii). From (H.2),

$$(H.8) \quad \frac{\bar{R}^{(k+1)}}{\bar{R}^{(k)}} = p + \frac{1}{\bar{R}^{(k)}} \sum_{j=1}^J s_j \max_{(k-M)_{++} \leq q \leq k} (\bar{R}^{(q)})^{\eta_j}.$$

For any  $q \in [(k-M)_{++}, k]$ , we have

$$(H.9) \quad \frac{(\bar{R}^{(q)})^{\eta_j}}{\bar{R}^{(k)}} = \frac{\bar{R}^{(q)}}{\bar{R}^{(k)}} (\bar{R}^{(q)})^{\eta_j-1} \leq \frac{\bar{R}^{(q)}}{\bar{R}^{(k)}} \left( \delta^{\lceil (q-1)/M \rceil} (bR^{(1)}) \right)^{\eta_j-1}.$$

Since  $\eta_j > 1$  and  $|q - k| \leq M$ , we have  $\delta^{\lceil (q-1)/M \rceil (\eta_j-1)} \rightarrow 0$  as  $k \rightarrow \infty$ , moreover as  $\bar{R}^{(k+1)}/\bar{R}^{(k)} \geq p$  for all  $k \geq 1$ ,  $\bar{R}^{(q)}/\bar{R}^{(k)} \leq p^{-M}$  for all  $q$ . Therefore, we get

$$(H.10) \quad \lim_{k \rightarrow \infty} \frac{\max_{(k-M)_{++} \leq q \leq k} (\bar{R}^{(q)})^{\eta_j}}{\bar{R}^{(k)}} = 0, \quad \forall j \implies \lim_{k \rightarrow \infty} \frac{\bar{R}^{(k+1)}}{\bar{R}^{(k)}} = p.$$

## REFERENCES

- [1] A. AGARWAL AND L. BOTTOU, *A lower bound for the optimization of finite sums*, in International Conference on Machine Learning, 2015, pp. 78–86.
- [2] Z. ALLEN-ZHU, *Katyusha: The first direct acceleration of stochastic gradient methods*, in Proceedings of the 49th Annual ACM SIGACT Symposium on Theory of Computing, STOC 2017, New York, NY, USA, 2017, ACM, pp. 1200–1205.
- [3] Y. ARJEVANI AND O. SHAMIR, *Dimension-free iteration complexity of finite sum optimization problems*, in Advances in Neural Information Processing Systems, 2016, pp. 3540–3548.
- [4] A. AYTEKIN, H. R. FEYZMAHDAVIAN, AND M. JOHANSSON, *Analysis and implementation of an asynchronous optimization algorithm for the parameter server*, arXiv preprint arXiv:1610.05507, (2016).
- [5] D. P. BERTSEKAS, *Nonlinear programming*, Athena scientific Belmont, 1999.
- [6] D. P. BERTSEKAS, *Incremental gradient, subgradient, and proximal methods for convex optimization: A survey*, Optimization for Machine Learning, 2010 (2011), p. 3.
- [7] D. BLATT, A. O. HERO, AND H. GAUCHMAN, *A convergent incremental gradient method with a constant step size*, SIAM Journal on Optimization, 18 (2007), pp. 29–51.
- [8] L. BOTTOU, F. E. CURTIS, AND J. NOCEDAL, *Optimization methods for large-scale machine learning*, arXiv preprint arXiv:1606.04838, (2016).
- [9] S. BUBECK ET AL., *Convex optimization: Algorithms and complexity*, Foundations and Trends® in Machine Learning, 8 (2015), pp. 231–357.
- [10] C.-C. CHANG AND C.-J. LIN, *LIBSVM: A library for support vector machines*, ACM Transactions on Intelligent Systems and Technology, 2 (2011), pp. 27:1–27:27. Software available at <http://www.csie.ntu.edu.tw/~cjlin/libsvm>.
- [11] A. DEFAZIO, F. BACH, AND S. LACOSTE-JULIEN, *Saga: A fast incremental gradient method with support for non-strongly convex composite objectives*, in NIPS, 2014, pp. 1646–1654.
- [12] H. R. FEYZMAHDAVIAN, A. AYTEKIN, AND M. JOHANSSON, *A delayed proximal gradient method with linear convergence rate*, in Machine Learning for Signal Processing (MLSP), 2014 IEEE International Workshop on, IEEE, 2014, pp. 1–6.
- [13] R. M. GOWER, N. L. ROUX, AND F. BACH, *Tracking the gradients using the hessian: A new look at variance reducing stochastic methods*, in AISTATS, April 2018.
- [14] M. GÜRBÜZBALABAN, A. OZDAGLAR, AND P. PARRILO, *A globally convergent incremental newton method*, Mathematical Programming, 151 (2015), pp. 283–313.
- [15] M. GÜRBÜZBALABAN, A. OZDAGLAR, AND P. PARRILO, *Why random reshuffling beats stochastic gradient descent*, arXiv preprint arXiv:1510.08560, (2015).
- [16] M. GÜRBÜZBALABAN, A. OZDAGLAR, AND P. PARRILO, *On the convergence rate of incremental aggregated gradient algorithms*, SIAM Journal on Optimization, 27 (2017), pp. 1035–1048.
- [17] G. LAN AND Y. ZHOU, *An optimal randomized incremental gradient method*, Mathematical programming, (2017), pp. 1–49.
- [18] H. LIN, J. MAIRAL, AND Z. HARCHAOU, *A universal catalyst for first-order optimization*, in Advances in Neural Information Processing Systems, 2015, pp. 3384–3392.
- [19] J. MAIRAL, *Incremental majorization-minimization optimization with application to large-scale machine learning*, SIAM Journal on Optimization, 25 (2015), pp. 829–855.
- [20] A. MOKHTARI, M. EISEN, AND A. RIBEIRO, *Iqn: An incremental quasi-newton method with local superlinear convergence rate*, arXiv preprint arXiv:1702.00709, (2017).
- [21] A. NEDIĆ AND D. BERTSEKAS, *Convergence rate of incremental subgradient algorithms*, in Stochastic optimization: algorithms and applications, Springer, 2001, pp. 223–264.
- [22] A. NEDIC AND D. P. BERTSEKAS, *Incremental subgradient methods for nondifferentiable optimization*, SIAM Journal on Optimization, 12 (2001), pp. 109–138.
- [23] Y. NESTEROV, *Introductory lectures on convex optimization: A basic course*, vol. 87, Springer Science & Business Media, 2013.
- [24] A. NITANDA, *Stochastic proximal gradient descent with acceleration techniques*, in Advances in Neural Information Processing Systems, 2014, pp. 1574–1582.
- [25] H. ROBBINS AND S. MONRO, *A stochastic approximation method*, The annals of mathematical statistics, (1951), pp. 400–407.
- [26] A. RODOMANOV AND D. KROPOTOV, *A superlinearly-convergent proximal newton-type method for the optimization of finite sums*, in International Conference on Machine Learning, 2016, pp. 2597–2605.
- [27] M. SCHMIDT, N. LE ROUX, AND F. BACH, *Minimizing finite sums with the stochastic average gradient*, Mathematical Programming, 162 (2017), pp. 83–112.
- [28] A. M.-C. SO AND Z. ZHOU, *Non-asymptotic convergence analysis of inexact gradient methods for machine learning without strong convexity*, Optimization Methods and Software, 32 (2017), pp. 963–992.
- [29] N. D. VANLI, M. GÜRBÜZBALABAN, AND A. OZDAGLAR, *A stronger convergence result on the proximal incremental aggregated gradient method*, arXiv preprint arXiv:1611.08022, (2016).
- [30] V. N. VAPNIK, *An overview of statistical learning theory*, IEEE transactions on neural networks, 10 (1999), pp. 988–999.
- [31] H.-T. WAI, W. SHI, A. NEDIĆ, AND A. SCAGLIONE, *Curvature-aided incremental aggregated gradient method*, in

- Proc. Allerton, October 2017.
- [32] L. XIAO AND T. ZHANG, *A proximal stochastic gradient method with progressive variance reduction*, SIAM Journal on Optimization, 24 (2014), pp. 2057–2075.